Density functional theory for disordered alloys with short-range order: Systematic inclusion of charge-correlation effects

D. A. Rowlands,[1] A. Ernst,[2] B. L. Györffy,[1] and J. B. Staunton[3]
[1]*H.H. Wills Physics Laboratory, University of Bristol, Bristol BS8 1TL, United Kingdom*
[2]*Max Planck Institut fr Mikrostrukturphysik, Weinberg 2, D-06120 Halle, Germany*
[3]*Department of Physics, University of Warwick, Coventry CV4 7AL, United Kingdom*
(Received 11 November 2005; revised manuscript received 17 January 2006; published 21 April 2006)

For many years, density-functional-based calculations for the total energies of substitutionally disordered alloys have been based upon the Korringa-Kohn-Rostoker coherent-potential approximation (KKR-CPA). However, as a result of the single-site nature of the KKR-CPA, such calculations do not take into account important local environmental effects such as charge correlations (the Madelung energy) and chemical short-range order (SRO). Here the above approach is generalized by combining the recently developed Korringa-Kohn-Rostoker nonlocal coherent-potential approximation with density functional theory, showing how these effects may be systematically taken into account. As a first application of the theory, total energy calculations for the bcc $Cu_{50}Zn_{50}$ solid solution are presented, showing how the total energy varies as a function of SRO. The fcc $Cu_{60}Pd_{40}$ and $Cu_{77}Ni_{23}$ systems are also investigated.

DOI: 10.1103/PhysRevB.73.165122 PACS number(s): 71.23.−k, 71.15.Mb, 71.15.Ap, 71.20.Be

I. INTRODUCTION

Many multicomponent metallic systems first crystallize into a solid solution and, as the temperature is lowered further, either order or phase separate.[1,2] A theory for this classic phenomenon of condensed matter physics can proceed in three possible ways. First, there is the phenomenological approach using Landau theory; second, there is the semiphenomenological approach using effective atomic potentials and classical statistical mechanics; or third, the problem can be tackled from first principles starting with the electrons and positively charged atomic nuclei.[2,3] These approaches can also be mixed; for example, multibody atomic potentials can be extracted from electronic total energy calculations for fixed configurations,[4] such procedures being the basis of much useful work on understanding phase diagrams.[2] However, here we are concerned with the third approach highlighted above which aims to treat the configurational statistical mechanics and the many-electron problem on more or less equal footing through to the end.[3,5] Such an approach is currently based upon the charge self-consistent Korringa-Kohn-Rostoker coherent-potential-approximation[6–10] (SCF-KKR-CPA) description of the disordered phase. The SCF-KKR-CPA is based on a density-functional-theory[11,12] (DFT) description of the electrons within the local density approximation (LDA) and uses the coherent-potential approximation[13] (CPA) to average over the ensemble of atomic configurations. It is this theory we wish to generalize by enabling the systematic inclusion of correlations between the occupations of the lattice sites.

Indeed, the principle shortcoming of the SCF-KKR-CPA, or its linear muffin-tin orbital (LMTO) derivatives,[14] is the fact that it results in the occupation variables ξ_i being treated as independent random variables. For a binary alloy these take on the value 0 or 1 depending on whether the site labeled by i is occupied by an A or B type of atom, respectively. This feature has two important and much discussed consequences. First, the entropy contribution to the free energy is restricted to the oversimplified Bragg-Williams logarithmic expression, the limitations of which are well documented by calculations using the cluster variational method.[15] Second, it forces each site, independently from the others, to be charge neutral on the average. Thus, as has been noted repeatedly in the literature (see, for example, Refs. 16–19), there is no Madelung contribution to the total energy. Despite numerous past successful applications of the SCF-KKR-CPA,[20,21] there is clearly a need for further conceptual development which takes into account configurational correlations.

The source of the above difficulties is the single-site nature of the conventional KKR-CPA (Refs. 22 and 23) in which an atom of a given chemical type only experiences the average effect of its environment. This automatically implies an "isomorphous"[24,25] model of the alloy in which all atoms of a given chemical type are assumed to be identical. In reality, for a given atomic configuration every site experiences a different environment and thus every site should have a different charge density and potential associated with it, after which the ensemble average over all atomic configurations should be taken. An effort to address this problem led to the development of the polymorphous coherent-potential approximation[25–28] (PCPA) based upon order-N methods,[29–31] requiring the use of large supercells and the single-site approximation in order to treat the Coulomb effects. Other recent methods include Refs. 32 and 33. However, an alternative way forward is provided by the recent appearance of the nonlocal CPA idea[34,35] and the subsequent development of the KKR-NLCPA,[36–38] a cluster theory which goes beyond the single-site approximation and hence is capable of averaging over correlated ensembles, while preserving the symmetries of the underlying lattice. Indeed, based on these developments, here a charge self-consistent SCF-KKR-NLCPA scheme is derived and presented. It is polymorphous in the sense that, in principle, for every cluster configuration each cluster site has a different potential associated with it, and so the theory is able to provide a system-

atic account of the Madelung energy. Moreover, the probabilities of the various cluster configurations can be biased to favor ordering or clustering, thus providing a description of short-range order (SRO).

As a final introductory remark, it is useful to clarify in more detail what is regarded as the "exact theory" to which the procedure derived here is an approximation. This will also highlight some of the conceptual ideas upon which the approach is based. First recall that the dynamics of alloy configurations is atomic diffusion. As this is a very slow process compared with the motion of the electrons, the "adiabatic approximation" with respect to such diffusion is virtually exact. Note that strain fluctuations or lattice vibrations are faster than diffusion but they are still slow enough to be treated adiabatically. Unfortunately, to do that one should allow the atoms to be displaced from the sites of the perfect (average) lattice positions. While the new theory to be presented here could deal with such static displacements,[39–41] their treatment is deferred to another publication.[42] Bearing in mind the above remarks, one may construct an exact theory by calculating the electronic grand potential $\Omega_e(\{\xi_i\})$ for each configuration $\{\xi_i\}$ and evaluating the partition function Z for the combined electron-atom system by summing over all configurations as follows:

$$Z = \sum_{\{\xi_i\}} \exp\left(\beta[\Omega_e(\{\xi_i\}) - \sum_i \nu_i \xi_i]\right), \tag{1}$$

where ν_i is the site-dependent chemical potential difference, thermodynamically conjugate to the local concentration c_i, and β is the usual dimensionless inverse temperature. Then the thermodynamic free energy $F(T,\nu) = -\frac{1}{\beta} \ln Z$ when $\nu_i = \nu$ for all i. Note that the electronic entropy associated with the thermal production of the electron hole pairs is included in $\Omega_e(\{\xi_i\})$ which is to be calculated exactly using DFT.

The point to focus on here is that the electronic grand potential $\Omega_e(\{\xi_i\})$ is given by a self-consistent one-electron theory and self-consistency with respect to the electronic charge distribution needs to be achieved before the sum over all configurations is taken. Both the SCF-KKR-CPA and the new SCF-KKR nonlocal coherent-potential approximation (NLCPA) make the doubly impossible tasks of calculating Z tractable by approximating the exact DFT by the LDA, widely used for ordered systems, and using the CPA or NLCPA, respectively, to sum over all configurations. The procedure is arrived at by inverting the order in which charge self-consistency is implemented and the average taken. In the case of the SCF-KKR-CPA, charge self-consistency is enforced only with respect to single-site partially averaged charge densities $\rho_A(\mathbf{r})$ and $\rho_B(\mathbf{r})$, such single-site partial averages being the constrained average over all configurations which leave the occupancy of a single site fixed. Remarkably, the free energy F is stationary with respect to $\rho_A(\mathbf{r})$ and $\rho_B(\mathbf{r})$,[9] which is arguably the main reason for the robust reliability of the method. As shown later, the new SCF-KKR-NLCPA is stationary with respect to arbitrary variations in the partially averaged cluster charge densities $\underline{\rho}_\gamma(\mathbf{r})$ which are defined for a cluster with fixed configuration γ, while the average over the occupancy of all other sites is taken. Evidently, these quantities are the direct generalizations of $\rho_A(\mathbf{r})$ and $\rho_B(\mathbf{r})$, this result being an attractive feature of the new theory.

The outline of this paper is as follows. First, in Secs. II A and II B the features of the KKR-NLCPA which will be needed in the subsequent discussion are recalled. Section II C explains how the total energy within the KKR-NLCPA may be derived based upon a generalized Lloyd formula. The need for defining cluster potential matrices $\underline{v}_\gamma(\mathbf{r})$ is described in detail in Sec. II D, and a specific form for $\underline{v}_\gamma(\mathbf{r})$ is chosen in Sec. II F which enables charge correlations within the range of the cluster to be systematically included into the total energy expression. In Sec. II G it is shown that this choice of potential maintains the stationary properties of DFT, thus establishing the charge self-consistency procedure outlined in Sec. II H. Results are given in Sec. III. Finally, conclusions are drawn and future work discussed in Sec. IV.

II. FORMALISM

A. Overview of the KKR-NLCPA

In order to go beyond an effective medium determined via a single-site theory such as the KKR-CPA, effective corrections $\underline{\widehat{\delta G}}(\mathbf{R}_{ij})$ to the usual free-space KKR structure constants $\underline{G}(\mathbf{R}_{ij})$ must be introduced. Thus the scattering path matrix $\underline{\hat{\tau}}^{ij}$ for a medium describing the average motion of an electron from site i to site j exactly is given by

$$\underline{\hat{\tau}}^{ij} = \underline{\hat{t}}\delta_{ij} + \sum_{k\neq i} \underline{\hat{t}}[\underline{G}(\mathbf{R}_{ik}) + \underline{\widehat{\delta G}}(\mathbf{R}_{ik})]\underline{\hat{\tau}}^{kj}. \tag{2}$$

Here a circumflex symbol denotes an effective medium quantity, an underscore denotes a matrix in angular momentum space, and the indices i,j run over all sites in the lattice. The effective scattering matrices are labeled by $\hat{t}$, and the effective structure constant corrections $\underline{\widehat{\delta G}}(\mathbf{R}_{ij})$ take into account all nonlocal scattering correlations due to the disorder configurations. Since the effective medium is translationally invariant, the matrix elements $\underline{\hat{\tau}}^{ij}$ are also given by the Brillouin zone integral

$$\underline{\hat{\tau}}^{ij} = \frac{1}{\Omega_{BZ}} \int_{\Omega_{BZ}} d\mathbf{k}[\underline{\hat{t}}^{-1} - \underline{G}(\mathbf{k}) - \underline{\widehat{\delta G}}(\mathbf{k})]^{-1} e^{i\mathbf{k}\cdot(\mathbf{R}_i - \mathbf{R}_j)}. \tag{3}$$

Since it is not feasible to solve the problem exactly, the key idea, based upon concepts from the dynamical cluster approximation (DCA),[34,43,44] is to map the problem to that of a self-consistently embedded impurity cluster problem, where the configurationally averaged impurity cluster has *periodic boundary conditions* imposed. This means that the range of nonlocal scattering correlations included in the medium is restricted by the size of the cluster, but significantly the full translational symmetry of the underlying lattice is retained. The key step is to solve the equation

$$\frac{1}{N_c} \sum_{\mathbf{K}_n} e^{i\mathbf{K}_n\cdot(\mathbf{R}_I - \mathbf{R}_J)} = \delta_{IJ}, \tag{4}$$

which, for a cluster of N_c sites with periodic boundary conditions, relates the real-space cluster sites $\{I,J\}$ (denoted by

capital letters) and the corresponding set of "cluster momenta" $\{\mathbf{K}_n\}$ with $n=1,\ldots,N_c$. The real-space cluster sites must be chosen so that they can be surrounded by a "tile"[34] which can be periodically repeated to fill out all space, in analogy to the conventional Wigner-Seitz cell used to surround a single site. The cluster momenta will correspondingly be centred at a set of N_c reciprocal-space tiles which divide up the first Brillouin zone of the lattice. However, as explained in Ref. 34, the principal lattice vectors of the chosen tiles must point along a high symmetry direction of the real lattice. This is to ensure that equivalent momenta lie in the same tile (when following the coarse-graining procedure outlined below), thus preserving the point-group symmetry of the underlying lattice. This restricts the allowed values of N_c for any given lattice. Full details of the general method for solving Eq. (4), including diagrams of the tiling and values of N_c, $\mathbf{R}_I$, and $\mathbf{K}_n$ for the commonly encountered bcc and fcc lattices, are given in Refs. 36–38.

We are now in a position to map the cluster problem to the lattice, which will first be done in reciprocal space. This is achieved by approximating $\underline{\widehat{\delta G}}(\mathbf{k})$ of Eq. (3) within each of the N_c tiles by the N_c "coarse-grained" values $\{\underline{\widehat{\delta G}}(\mathbf{K}_n)\}$, each defined to be the average of $\underline{\widehat{\delta G}}(\mathbf{k})$ over the tile centered at $\mathbf{K}_n$. Then by using Eq. (4) we have

$$\underline{\widehat{\delta G}}(\mathbf{R}_{IJ}) = \frac{1}{N_c}\sum_{\mathbf{K}_n} \underline{\widehat{\delta G}}(\mathbf{K}_n) e^{i\mathbf{K}_n\cdot(\mathbf{R}_I-\mathbf{R}_J)},$$

$$\underline{\widehat{\delta G}}(\mathbf{K}_n) = \sum_{J\neq I} \underline{\widehat{\delta G}}(\mathbf{R}_{IJ}) e^{-i\mathbf{K}_n\cdot(\mathbf{R}_I-\mathbf{R}_J)}. \tag{5}$$

Note that $\underline{\widehat{\delta G}}(\mathbf{R}_{IJ})$ remains a translationally invariant quantity which depends only on the distance between sites I and J, now within the range of the cluster size, but independent of which site in the lattice is chosen to be site I. The scattering path matrix may now be represented by the set of coarse-grained values

$$\hat{\underline{\tau}}(\mathbf{K}_n) = \frac{N_c}{\Omega_{BZ}}\int_{\Omega_{\mathbf{K}_n}} d\mathbf{k}[\hat{\underline{t}}^{-1} - \underline{G}(\mathbf{k}) - \underline{\widehat{\delta G}}(\mathbf{K}_n)]^{-1}, \tag{6}$$

which are straightforward to calculate since $\underline{\widehat{\delta G}}(\mathbf{K}_n)$ is constant within each tile $\Omega_{\mathbf{K}_n}$. Using Eq. (4), the scattering path matrix at the cluster sites becomes

$$\hat{\underline{\tau}}^{IJ} = \frac{1}{\Omega_{BZ}}\sum_{\mathbf{K}_n}\left(\int_{\Omega_{\mathbf{K}_n}} d\mathbf{k}[\hat{\underline{t}}^{-1} - \underline{G}(\mathbf{k}) - \underline{\widehat{\delta G}}(\mathbf{K}_n)]^{-1}\right) \times e^{i\mathbf{K}_n\cdot(\mathbf{R}_I-\mathbf{R}_J)}. \tag{7}$$

The final step is to determine the medium by generalizing the KKR-CPA argument in real space. First note that for paths starting and ending on the sites of the chosen cluster, Eq. (2) may be rearranged in the form

$$\hat{\underline{\tau}}^{IJ} = \hat{\underline{t}}_{cl}^{IJ} + \sum_{K,L} \hat{\underline{t}}_{cl}^{IK}\hat{\underline{\Delta}}^{KL}\hat{\underline{\tau}}^{LJ}, \tag{8}$$

where the effective cluster t matrix is defined by

$$\hat{\underline{t}}_{cl}^{IJ} = \hat{\underline{t}}^{I}\delta_{IJ} + \sum_{K} \hat{\underline{t}}^{I}[\underline{G}(\mathbf{R}_{IK}) + \underline{\widehat{\delta G}}(\mathbf{R}_{IK})]\hat{\underline{t}}_{cl}^{KJ} \tag{9}$$

and describes all scattering within the cluster, while the cluster renormalized interactor[45,46] or cavity propagator $\hat{\underline{\Delta}}^{IJ}$ describes all scattering outside of the cluster. Since $\bar{\underline{\Delta}}^{IJ}$ describes the medium outside and is independent of the contents of the cluster, it may be used to define the impurity cluster path matrix

$$\underline{\tau}_{\gamma}^{IJ} = \underline{t}_{cl,\gamma}^{IJ} + \sum_{K,L} \underline{t}_{cl,\gamma}^{IK}\hat{\underline{\Delta}}^{KL}\underline{\tau}_{\gamma}^{LJ}, \tag{10}$$

where the impurity cluster t matrix is defined by

$$\underline{t}_{cl,\gamma}^{IJ} = \underline{t}_{\gamma}^{I}\delta_{IJ} + \sum_{K} \underline{t}_{\gamma}^{I}\underline{G}(\mathbf{R}_{IK})\underline{t}_{cl,\gamma}^{KJ} \tag{11}$$

for a fixed impurity cluster configuration γ. In other words, the effective cluster has simply been replaced by an "impurity" cluster of real t matrices with configuration γ and free-space structure constants "embedded" in the (still undetermined) effective medium. The KKR-NLCPA self-consistency condition demands that there be no additional scattering from the cluster on the average—i.e.,

$$\sum_{\gamma} P_{\gamma}\underline{\tau}_{\gamma}^{IJ} = \hat{\underline{\tau}}^{IJ}, \tag{12}$$

where P_{γ} is the probability of configuration γ occurring. The effective medium t matrices and structure constant corrections are thus determined from a self-consistent solution of Eqs. (7) and (12). An example algorithm is given in Refs. 36 and 37. Note that the cluster probabilities depend on the SRO parameter α—i.e., $P_{\gamma}=P_{\gamma}[\alpha]$ and so SRO may be included by appropriately weighting the configurations in Eq. (12) provided that translational invariance is preserved. Finally note that the KKR-NLCPA formalism reduces to the KKR-CPA for $N_c=1$ and becomes exact as $N_c\to\infty$.

B. Calculating properties

As a generalization of the approach adopted by Faulkner and Stocks[47] for calculating properties within the conventional KKR-CPA, observe that one may formally write down an expression for the exact *cluster restricted-average* Green's function—i.e., the Green's function for which a cluster of configuration γ is kept fixed, but the average is taken over all possible configurations outside. This is given by

$$\langle \underline{\underline{G}}(\mathbf{r},\mathbf{r}',E)\rangle_{\gamma} = \underline{\underline{Z}}_{\gamma}(\mathbf{r},E)\langle \underline{\underline{\tau}}(E)\rangle_{\gamma}\underline{\underline{Z}}_{\gamma}(\mathbf{r}',E) - \underline{\underline{Z}}_{\gamma}(\mathbf{r},E)\underline{\underline{J}}_{\gamma}(\mathbf{r}',E)\delta_{IJ}, \tag{13}$$

where the double underscore denotes a matrix in both the cluster-site and angular momentum index, and $\mathbf{r},\mathbf{r}'$ can lie anywhere within the cluster. The matrices $\underline{\underline{Z}}_{\gamma}$ and $\underline{\underline{J}}_{\gamma}$ are diagonal in the cluster-site index, and for a fixed cluster configuration γ they have site-matrix elements given by the regular and irregular solutions, respectively, of the single-site problem at that site. As an example, for a two-site cluster of configuration $\gamma=AB$ with A at I and B at J, we have

$$\underline{\underline{Z}}_\gamma(\mathbf{r},E)=\begin{bmatrix}\underline{Z}_A(\mathbf{r}_I,E) & 0\\ 0 & \underline{Z}_B(\mathbf{r}_J,E)\end{bmatrix},$$

$$\underline{\underline{J}}_\gamma(\mathbf{r},E)=\begin{bmatrix}\underline{J}_A(\mathbf{r}_I,E) & 0\\ 0 & \underline{J}_B(\mathbf{r}_J,E)\end{bmatrix}, \tag{14}$$

where $\mathbf{r}_I$ implies that $\mathbf{r}$ is restricted to lie within site I and is measured from the nuclear position $\mathbf{R}_I$. Similarly $\mathbf{r}_J$ is restricted to lie within site J and is measured from $\mathbf{R}_J$. Adopting this notation, a site-matrix element of Eq. (13) is given by

$$\langle \underline{G}(\mathbf{r}_I,\mathbf{r}'_J,E)\rangle_\gamma=\underline{Z}_\gamma(\mathbf{r}_I,E)\langle \underline{\tau}^{JJ}(E)\rangle_\gamma \underline{Z}_\gamma(\mathbf{r}'_J,E) - \underline{Z}_\gamma(\mathbf{r}_I,E)\underline{J}_\gamma(\mathbf{r}'_J,E)\,\delta_{IJ}, \tag{15}$$

where a single underscore denotes a matrix in the angular momentum index only.

Within the KKR-NLCPA, for each cluster configuration γ the exact cluster restricted average is approximated by using an impurity cluster of configuration γ embedded in the KKR-NLCPA effective medium. In other words, Eq. (15) becomes

$$\underline{G}_\gamma(\mathbf{r}_I,\mathbf{r}'_J,E)=\underline{Z}_\gamma(\mathbf{r}_I,E)\underline{\tau}^{JJ}_\gamma\underline{Z}_\gamma(\mathbf{r}'_J,E)-\underline{Z}_\gamma(\mathbf{r}_I,E)\underline{J}_\gamma(\mathbf{r}'_J,E)\,\delta_{IJ}, \tag{16}$$

where $\underline{\tau}^{JJ}_\gamma$ is the impurity cluster path matrix given by Eq. (10). Let us now restrict the discussion to the calculation of site-diagonal properties only. For a fixed cluster configuration γ, the component density of states (DOS) and component charge density measured at any particular cluster site I are given by the expressions

$$n^I_\gamma(E)=-\frac{1}{\pi}\,Im\int d\mathbf{r}_I\sum_{LL'}[\underline{G}_\gamma(\mathbf{r}_I,\mathbf{r}_I,E)]_{LL'}, \tag{17}$$

$$\rho_\gamma(\mathbf{r}_I)=-\frac{1}{\pi}\,Im\int_{-\infty}^{\mu}dE\sum_{LL'}[\underline{G}_\gamma(\mathbf{r}_I,\mathbf{r}_I,E)]_{LL'}, \tag{18}$$

respectively. The total configurationally averaged DOS and charge density per site are simply given by

$$\bar{n}(E)=\sum_\gamma P_\gamma n^I_\gamma(E), \tag{19}$$

$$\bar{\rho}(\mathbf{r}_I)=\sum_\gamma P_\gamma \rho_\gamma(\mathbf{r}_I), \tag{20}$$

respectively, where P_γ is the probability of configuration γ occurring and any site I in the cluster may be chosen since all sites are equivalent on the average. The integral over $\mathbf{r}_I$ above can be taken over the conventional unit cell at site I. This is because, through symmetry, the space enclosed by the conventional Wigner-Seitz cells surrounding the cluster sites is equivalent to that enclosed by the "tile" used to define the cluster as described in the previous section.

C. Total energy within the KKR-NLCPA

By integrating Maxwell's relation $N=-(\partial\Omega/\partial\mu)$ for a fixed configuration where N is the number of electrons, it can be shown that the fundamental equation for the configurationally averaged electronic grand potential is given by[8,9]

$$\bar{\Omega}=\mu\bar{N}(\mu,\mu)-\int_{-\infty}^{\mu}dE\bar{N}(E,\mu)+\int_{-\infty}^{\mu}d\mu'\int_{-\infty}^{\mu'}dE\frac{\delta\bar{N}(E,\mu')}{\delta\mu'}, \tag{21}$$

where $\bar{N}$ is the configurationally averaged integrated density of states per site at constant temperature and volume, and μ is the electronic chemical potential. Adding the energy of the ion-ion interactions to $\bar{\Omega}$ gives the total internal energy of the system. The significance of the above equation is that only an approximation for $\bar{N}$ is required, albeit for all values of μ, and in the case of the KKR-CPA this is readily obtained from the KKR-CPA Lloyd formula.[48,49] Similarly, in order to derive an electronic grand potential Ω within the KKR-NLCPA, we need an expression for $\bar{N}$ and its variation with respect to the chemical potential $\delta\bar{N}/\delta\mu$. Within the KKR-NLCPA, it can be straightforwardly shown that $\bar{N}$ is given by the generalized Lloyd formula

$$\bar{N}(E,\mu)=N_0(E)-\frac{1}{\pi}\frac{1}{\Omega_{BZ}}\times\mathrm{Im}\left[\sum_{\mathbf{K}_n}\int_{\Omega_{\mathbf{K}_n}}d\mathbf{k}\,\ln\|\hat{\underline{t}}^{-1}-\widehat{\underline{\delta G}}(\mathbf{K}_n)-\underline{G}(\mathbf{k})\|\right] - \frac{1}{\pi N_c}\mathrm{Im}\left[\sum_\gamma P_\gamma\ln\|\underline{\underline{\tau}}^{-1}_\gamma\|-\ln\|\hat{\underline{\underline{\tau}}}^{-1}\|\right], \tag{22}$$

where $\hat{t}^{-1}$ and $\widehat{\delta G}(\mathbf{K}_n)$ are the effective medium single-site scattering t-matrix and reciprocal-space structure constant corrections, respectively, $\underline{G}(\mathbf{k})$ are the free-space structure constants, N_c is the number of sites in the cluster, and N_0 is the free-electron contribution. The determinants in the final term are over both the angular momentum and cluster-site indices. By combining Eqs. (8) and (10), the impurity and effective cluster scattering path matrices $\underline{\underline{\tau}}_\gamma$ and $\hat{\underline{\underline{\tau}}}$ are related by

$$\underline{\underline{\tau}}^{-1}_\gamma=\underline{\underline{t}}^{-1}_{cl,\gamma}-\hat{\underline{\underline{t}}}^{-1}_{cl}+\hat{\underline{\underline{\tau}}}^{-1}, \tag{23}$$

where $\hat{\underline{\underline{t}}}_{cl}$ and $\underline{\underline{t}}_{cl,\gamma}$ are the effective and impurity cluster t matrices given by Eqs. (9) and (11), respectively.

The aim is now to evaluate $d\bar{N}/d\mu$ and hence obtain an expression for the electronic grand potential within the KKR-NLCPA. As a consequence of the general form of the KKR-NLCPA Lloyd formula above, central to the derivation will be the *cluster potential* and *cluster charge density* matrices as described in the next section.

D. Cluster potentials and cluster component charge densities

As detailed in Sec. II B, in the KKR-NLCPA we may calculate *cluster component densities of states* and *cluster component charge densities* measured at any particular cluster site, as given by Eqs. (17) and (18), respectively. These should be viewed as approximations to the corresponding

exact cluster restricted-average quantities. They are calculated by first determining the effective medium using a cluster of size N_c and then reembedding the appropriate impurity cluster configuration back into the medium. We may pick any cluster site—say, I—and measure the DOS or charge density at that site using the impurity cluster path matrix $\underline{\tau}_{\gamma}^{II}$, where γ is the configuration of the cluster. Clearly, when site I is, say, an A site, the component DOS and charge density measured at site I will be different depending on the remaining configuration of the cluster (see the results in Ref. 38). This is a direct consequence of the fact that $\underline{\tau}_{\gamma}^{II}$ contains information about the local environment surrounding site I for the fixed configuration γ.

Next recall that in the conventional single-site KKR-CPA, single-site potentials may be defined in terms of the single-site component charge densities.[6–8] In order to proceed further in deriving the electronic grand potential and obtaining self-consistent potentials within the KKR-NLCPA, we need to define a set of *cluster potentials* in terms of the set of cluster component charge densities (the precise relation will be given later in Sec. II F). From the discussion above, it is clear that for a fixed configuration γ, each of the N_c sites will in principle have a different potential associated with them. In other words, the Kohn-Sham equation will in principle need to be solved $2^{N_c} \times N_c$ times for a binary alloy.

In the interest of clarity we now introduce the following notation. By measuring the cluster component charge density via Eq. (18) at each site in the cluster, we may define the cluster component charge density matrix $\underline{\rho}_{\gamma}(\mathbf{r})$ such that

$$[\underline{\rho}_{\gamma}(\mathbf{r})]_{II} = \rho_{\gamma}(\mathbf{r}_I),$$

where as usual $\mathbf{r}_I$ implies that $\mathbf{r}$ restricted to lie within site I and is measured from the nuclear position $\mathbf{R}_I$. Similarly, we introduce the cluster potential matrix $\underline{v}_{\gamma}(\mathbf{r})$ with site matrix elements

$$[\underline{v}_{\gamma}(\mathbf{r})]_{II} = v_{\gamma}(\mathbf{r}_I).$$

As an example, for the simple case of a two-site cluster for a binary alloy we will have $2^2=4$ cluster potential and cluster component charge density matrices and will have $2^2 \times 2 = 8$ distinct single-site potentials. For the configuration $\gamma=\{AB\}$ we have

$$\underline{v}_{\gamma}(\mathbf{r}) = \begin{bmatrix} v_{AB}(\mathbf{r}_I) & 0 \\ 0 & v_{AB}(\mathbf{r}_J) \end{bmatrix},$$

$$\underline{\rho}_{\gamma}(\mathbf{r}) = \begin{bmatrix} \rho_{AB}(\mathbf{r}_I) & 0 \\ 0 & \rho_{AB}(\mathbf{r}_J) \end{bmatrix}.$$

Although the potentials are single-site quantities, it is still necessary to include the full configuration label. This is because although, for example, $v_{AB}(\mathbf{r}_J)$ is a "B" site, $v_{AB}(\mathbf{r}_J)$ is not the same single-site potential as $v_{BB}(\mathbf{r}_J)$. The same notation must also be applied to the corresponding wave functions and cluster t matrices when attempting to obtain self-consistent potentials; i.e., Eq. (14) becomes

$$\underline{\underline{Z}}_{\gamma} = \begin{bmatrix} \underline{Z}_{AB}(\mathbf{r}_I, E) & 0 \\ 0 & \underline{Z}_{AB}(\mathbf{r}_J, E) \end{bmatrix}$$

and the cluster t matrix becomes

$$\underline{\underline{t}}_{cl,\gamma} = \begin{bmatrix} \underline{t}_{AB}^{I} & \underline{G}(\mathbf{R}_{IJ}) \\ \underline{G}(\mathbf{R}_{JI}) & \underline{t}_{AB}^{J} \end{bmatrix}$$

for $\gamma=\{AB\}$.

E. Electronic grand potential

Using the cluster component charge densities and cluster potentials described in the previous section together with Eq. (22), it is now possible to derive an expression for $d\bar{N}/d\mu'$, as shown in Appendix B. Having done this, Eq. (21) becomes

$$\bar{\Omega} = \mu \bar{N}(\mu,\mu) - \int_{-\infty}^{\mu} dE \bar{N}(E,\mu) - \frac{1}{N_c}\int_{-\infty}^{\mu} d\mu' \sum_{\gamma} P_{\gamma} \sum_{I} \left(\int d\mathbf{r}_I \rho_{\gamma}(\mathbf{r}_I,\mu') \frac{\partial v_{\gamma}(\mathbf{r}_I,\mu')}{\partial \mu'} \right). \tag{24}$$

By performing the integration with respect to μ' by parts, an expression for the electronic grand potential in terms of potentials and electronic charge densities is obtained in the form

$$\bar{\Omega} = \mu \bar{N}(\mu,\mu) - \int_{-\infty}^{\mu} dE \bar{N}(E,\mu) - \frac{1}{N_c}\sum_{\gamma} P_{\gamma} \sum_{I} \left(\int d\mathbf{r}_I \rho_{\gamma}(\mathbf{r}_I,\mu) v_{\gamma}(\mathbf{r}_I,\mu) \right) + \frac{1}{N_c}\int_{-\infty}^{\mu} d\mu' \sum_{\gamma} P_{\gamma} \sum_{I} \left(\int d\mathbf{r}_I v_{\gamma}(\mathbf{r}_I,\mu') \frac{d\rho_{\gamma}(\mathbf{r}_I,\mu')}{d\mu'} \right). \tag{25}$$

This is the cluster generalization of Eq. (9) in Ref. 9. In the next section a specific form for $\underline{v}_{\gamma}(\mathbf{r})$ is chosen. In particular it is shown that this choice enables charge correlations within the range of the cluster to be systematically included in the total energy expression. Furthermore, it will subsequently be shown that this choice of potential maintains the stationary properties of DFT, thus establishing the charge self-consistency procedure outlined in Sec. II H.

F. Choice of local potential: Systematic inclusion of charge correlations

For a particular cluster configuration γ, we choose the cluster potential $\underline{v}_{\gamma}(\mathbf{r})$ within a cluster site I to take the form

$$v_\gamma(\mathbf{r}_I) = \sum_J \int d\mathbf{r}'_J \frac{\rho_\gamma(\mathbf{r}'_J)}{|\mathbf{r}_I - \mathbf{r}'_J + \mathbf{R}_{IJ}|} - \sum_J \frac{Z^J_\gamma}{|\mathbf{r}_I + \mathbf{R}_{IJ}|} + \sum_{n\notin C} \int d\mathbf{r}'_n \frac{\bar{\rho}(\mathbf{r}'_n)}{|\mathbf{r}_I - \mathbf{r}'_n + \mathbf{R}_{In}|} - \sum_{n\notin C} \frac{\bar{Z}^n}{|\mathbf{r}_I + \mathbf{R}_{In}|} + v^{xc}_\gamma[\rho_\gamma(\mathbf{r}_I)], \tag{26}$$

where the sums in the first two terms are over all sites J (including $J=I$) belonging to the cluster and the sums in the third and fourth terms are over all sites n outside of the cluster. Notation has been introduced such that the nuclear charge on a cluster site I for the fixed cluster configuration γ is labeled as Z^I_γ. The average charge and nuclear densities placed on all sites outside the cluster are given by

$$\bar{\rho}(\mathbf{r}_n) = \frac{1}{N_c}\sum_I \sum_\gamma P_\gamma \rho_\gamma(\mathbf{r}_I) = \sum_\gamma P_\gamma \rho_\gamma(\mathbf{r}_I), \tag{27}$$

$$\bar{Z}^n = \frac{1}{N_c}\sum_I \sum_\gamma P_\gamma Z^I_\gamma = \sum_\gamma P_\gamma Z^I_\gamma. \tag{28}$$

Here the sum over all cluster sites I may be removed since all sites are equivalent after averaging over all cluster configurations, a consequence of translational invariance (see Appendix E).

In Eq. (26), the first and second terms represent the electronic and nuclear Coulomb contribution, respectively, at $\mathbf{r}_I$ from each site in the cluster for the fixed configuration γ. The third and fourth terms represent the average electronic and nuclear contribution from all sites outside of the impurity cluster. Although each site is neutral on the average due to translational invariance (but *not independently from the other sites* as in the KKR-CPA), we have $\int d\mathbf{r}_n \bar{\rho}(\mathbf{r}_n) - \bar{Z}^n = 0$. However, these terms should still be included as there is in general a multipole contribution arising from them. The final term represents the exchange correlation potential[11,12] at $\mathbf{r}_I$, given that the impurity cluster configuration is γ.

Now inserting Eq. (26) into the final term of Eq. (25) and performing the integration with respect to μ' by parts (see Appendix C) leads to the expression for the electronic grand potential in the form

$$\bar{\Omega} = \mu \bar{N}(\mu,\mu) - \int_{-\infty}^{\mu} dE \bar{N}(E,\mu) - \frac{1}{N_c}\sum_\gamma P_\gamma \sum_I \int d\mathbf{r}_I \rho_\gamma(\mathbf{r}_I,\mu) v_\gamma(\mathbf{r}_I,\mu) + \frac{1}{2}\frac{1}{N_c}\sum_\gamma P_\gamma \sum_{I,J} \frac{\int d\mathbf{r}_I \rho_\gamma(\mathbf{r}_I) \int d\mathbf{r}'_J \rho_\gamma(\mathbf{r}'_J)}{|\mathbf{r}_I - \mathbf{r}'_J + \mathbf{R}_{IJ}|} - \frac{1}{N_c}\sum_\gamma P_\gamma \sum_{I,J} \frac{\int d\mathbf{r}_I \rho_\gamma(\mathbf{r}_I) Z^J_\gamma}{|\mathbf{r}_I + \mathbf{R}_{IJ}|} + \frac{1}{2}\frac{1}{N_c}\sum_\gamma P_\gamma \sum_I \sum_{n\notin C} \frac{\int d\mathbf{r}_I \rho_\gamma(\mathbf{r}_I) \int d\mathbf{r}'_n \bar{\rho}(\mathbf{r}'_n)}{|\mathbf{r}_I - \mathbf{r}'_n + \mathbf{R}_{In}|} - \frac{1}{N_c}\sum_\gamma P_\gamma \sum_I \sum_{n\notin C} \frac{\int d\mathbf{r}_I \rho_\gamma(\mathbf{r}_I) \bar{Z}^n}{|\mathbf{r}_I + \mathbf{R}_{In}|} + \frac{1}{N_c}\sum_\gamma P_\gamma \sum_I \int d\mathbf{r}_I \rho_\gamma(\mathbf{r}_I) v^{xc}_\gamma[\rho_\gamma(\mathbf{r}_I)]. \tag{29}$$

In the above expression the first three terms represent the configurationally averaged kinetic energy. It can be seen that the fourth and fifth terms involve Coulomb interactions between all cluster sites for each fixed impurity configuration γ resulting from the fact that there will be a net (and different) overall charge on each cluster site. After the average over all configurations γ is taken, charge neutrality will be restored; however, we have gained an energy contribution

$$\bar{\Omega}^{(4,5)} = \frac{1}{2}\frac{1}{N_c}\sum_\gamma P_\gamma \sum_{I,J} \frac{\int d\mathbf{r}_I \rho_\gamma(\mathbf{r}_I)[\int d\mathbf{r}'_J \rho_\gamma(\mathbf{r}'_J) - 2Z^J_\gamma]}{|\mathbf{r}_I - \mathbf{r}'_J + \mathbf{R}_{IJ}|}. \tag{30}$$

The off-diagonal part of Eq. (30) above (i.e., when $J \neq I$) arises from charge correlations between the cluster sites, such terms being absent in the conventional single-site KKR-CPA expression. An estimate of the Madelung contribution to the total internal energy per site, which is missing in the single-site KKR-CPA,[16–19] may therefore be calculated by excluding the $J=I$ terms from the above summation, yielding

$$E_M = \frac{1}{2}\frac{1}{N_c}\sum_\gamma P_\gamma \sum_{I,J\neq I} \frac{\int d\mathbf{r}_I \rho_\gamma(\mathbf{r}_I)[\int d\mathbf{r}'_J \rho_\gamma(\mathbf{r}'_J) - 2Z^J_\gamma]}{|\mathbf{r}_I - \mathbf{r}'_J + \mathbf{R}_{IJ}|}. \tag{31}$$

The sixth and seventh terms in Eq. (29) represent the contributions from the average electronic and nuclear charges outside the cluster. The last term is the exchange-correlation energy.[11,12] Finally, it is important to appreciate that charge neutrality will always be restored after averaging over all the cluster configurations since the SCF-KKR-NLCPA is, by construction, a translationally invariant theory. Indeed, Appendix E explains how translational invariance may be used to rewrite Eq. (29) in a simplified form.

It is also worth pointing out that earlier methods[50,51] to include charge-transfer effects by attempting to correct the SCF-KKR-CPA results within the single-site framework do not provide a satisfactory treatment of the electrostatic energy.[52] However, the treatment presented above is a natural and systematic way of bridging the gap between the SCF-KKR-CPA and the exact result.

G. Stationary properties

In DFT for usual systems the total energy or Ω is a functional of the charge density and, furthermore, is stationary

with respect to the ground-state charge density with the condition that the number of particles, N, is kept constant. The total energy within the KKR-CPA maintains this variational property since Ω is stationary with respect to the partially averaged charge densities $\rho_\alpha(\mathbf{r})$, where α is the atomic species—i.e., $\delta\{\Omega-\mu\bar{N}\}/\delta\rho_\alpha(\mathbf{r})=0$.[9]

It is desirable that the total energy within the KKR-NLCPA be variational. This is shown to be the case in Appendix D, where it is proven that $\delta\{\Omega-\mu\bar{N}\}/\delta(\rho_\gamma(\mathbf{r}_I))=0$ for each cluster configuration γ where $\mathbf{r}_I$ is a point within any cluster site I. This variational property arises from the combined effects of the variational properties of DFT and the KKR-NLCPA, and establishes the charge self-consistency procedure outlined in Sec. II H.

H. Charge self-consistency

It is now appropriate to summarize the steps involved in obtaining charge self-consistency.

(i) Begin with an appropriate guess for the set of 2^{N_c} cluster potential matrices $\underline{v}_\gamma(\mathbf{r})$.

(ii) Calculate the corresponding cluster t matrices and use the KKR-NLCPA to determine the effective medium.

(iii) Calculate the site-diagonal part of the partially averaged cluster Green's functions $\underline{\underline{G}}_\gamma(\mathbf{r},\mathbf{r})$ and from these calculate the corresponding partially averaged cluster charge densities $\underline{\rho}_\gamma(\mathbf{r})$.

(iv) Using the charge densities above, reconstruct new cluster potentials $\underline{v}_\gamma(\mathbf{r})$. For a particular configuration γ, this is given by Eq. (26) for $\mathbf{r}$ lying within site I. This needs to be calculated for each I with $I=1,\ldots,N_c$ for the configuration γ.

(v) Compare with the previous cluster potentials and iterate to self-consistency.

To clarify the above rather complex procedure, the simple example of a binary alloy with $N_c=2$ is considered explicitly in Appendix F.

III. RESULTS

As a first illustration of the new SCF-KKR-NLCPA theory, results are presented here for the CuZn, CuPd and CuNi systems. Note that the SCF-KKR-NLCPA derivation presented in this paper has not made any assumption about the particular form for the local potentials. The calculations presented here use a full charge approximation approach [see Ref. 53, except that we use Voronoi cell geometry instead of the atomic sphere approximation (ASA) for the charge density and the effective potential as implemented in, for example, Ref. 54]. In order to obtain accurate total energies, the Lloyd formula must be used to calculate the integrated DOS and determine the Fermi level. By manipulating Eq. (22), we use a generalization of the form introduced in Ref. 55. Details of manipulating the equations for the local potentials Eq. (26) and grand potential Eq. (29) into a tractable form are given in Appendix G. The resulting expressions are implemented here within the scheme introduced in Ref. 56.

A. $Cu_{50}Zn_{50}$ (bcc)

A detailed investigation of the effects of SRO on the DOS of the $Cu_{50}Zn_{50}$ system using the (non-SCF) KKR-NLCPA with $N_c=2$ has been carried out in Ref. 38. However, the calculations of Ref. 38 used potentials from an SCF-KKR-CPA calculation; in other words, it was not possible to enforce charge self-consistency with respect to the KKR-NLCPA medium. This means there was only a one-component Cu and one-component Zn potential, and so the effects of charge transfer between the cluster sites were neglected. Furthermore, only the effects of SRO on the band energy could in principle be investigated. In contrast, using the new SCF-KKR-NLCPA theory, full total energy calculations may now be performed which take into account SRO. In the case of $Cu_{50}Zn_{50}$ with $N_c=2$, we now have two distinct Cu and two distinct Zn potentials, each with either a Cu or Zn neighbor. Possible charge transfer is therefore take into account, and we also have a Madelung contribution to the total energy.

First let us consider the case of $\alpha=0$—i.e., no SRO. In order for accurate comparisons to be made, Fig. 1(a) shows a repeat of the $N_c=2$ non-SCF KKR-NLCPA DOS calculation for $Cu_{50}Zn_{50}$ first given in Ref. 38 but using the full charge density approximation for the local potentials and an energy contour with 5 mRy imaginary part. First note that there is little observable difference in the total DOS compared with the SCF-KKR-CPA calculation given in the same figure. This is expected as the size of the cluster is very small, and the difference due to the nonlocal scattering correlations shows up in detail only on a scale of ±1 state/atom/Ry (see the diagram in Ref. 38). Nevertheless, in a dramatic departure from the conventional SCF-KKR-CPA calculation where only single-site Cu and Zn components exist, here the component contributions from the four possible cluster configurations are apparent. The component plots here are the DOS measured at the first cluster site [using Eq. (17)] when a particular cluster configuration is "embedded" in the KKR-NLCPA medium, which is the Cu site for the Cu–Cu and Cu–Zn configurations and the Zn site for the Zn–Cu and Zn–Zn configurations. Crucially, owing to the translational invariance of the KKR-NLCPA medium as described earlier, measurement at the second site gives the same results with a simple reversal of the labels of the Cu–Zn and Zn–Cu components [see Eq. (F1)]. Figure 1(b) shows a new SCF-KKR-NLCPA calculation for the same system with $\alpha=0$. It is clear that there is now an observable difference between the total DOS results using the SCF-KKR-NLCPA compared to the SCF-KKR-CPA. This difference is plotted in Fig. 1(c) and integrates to zero since there are the same number of electrons (11.5) per site in both cases (the Fermi level has been subtracted separately for each total DOS plot in Fig. 1). As can be seen by examining the corresponding component DOS plots, this difference arises from charge transfer between the cluster sites at certain energy regions. Here the energy regions in which this occurs are well separated since $Cu_{50}Zn_{50}$ is in the "split-band" regime. For example, for the peaks centered at approximately −0.2 Ry, the difference between the Cu–Cu and Cu–Zn components increases; i.e., they become more unlike each other. Similarly, for the peaks

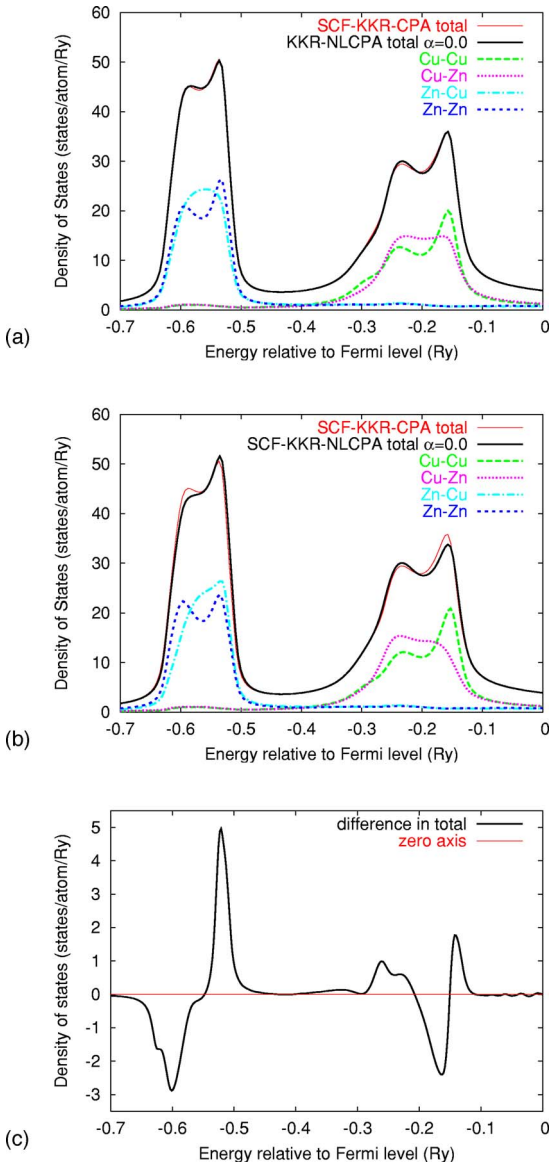

FIG. 1. (Color online) (a) Total average DOS for disordered bcc $Cu_{50}Zn_{50}$ using both the SCF-KKR-CPA and the KKR-NLCPA (non-SCF) with $N_c=2$. Also shown are the contributions from the four possible cluster configurations measured at the first site—i.e., Cu for Cu–Cu, Cu–Zn and Zn for Zn–Cu, Zn–Zn. (Owing to translational invariance, measurement at the second site would give the same results with a simple reversal of the labels.) (b) Same as above but using the new self-consistent-field (SCF)-KKR-NLCPA. (c) Plot of the difference between the total SCF-KKR-CPA and total SCF-KKR-NLCPA results.

centered at approximately −0.15 Ry, the Zn−Cu and Zn−Zn components become more unlike each other, all as a result of charge transfer.

Now let us consider the total energy of the system. Figure 4(c), below, shows that there is an overall lowering of the total energy (of order 0.28 mRy) calculated using the SCF-KKR-NLCPA for $\alpha=0.0$ compared with the SCF-KKR-CPA calculation. The Madelung contribution to the total energy calculated via Eq. (31) or Eq. (E2) is −2.41 mRy. This compares favorably with values of −2.5 mRy and −2.67 mRy previously obtained using large supercell calculations in Refs. 31 and 57, respectively. Of course, the reason why the difference in the total energy is much smaller is that changes in the potential contribution to the total energy are largely compensated for by corresponding changes in the kinetic contribution when the Madelung term is included in such self-consistent calculations, as is evident from Fig. 1(b).

Now we introduce the nearest-neighbor SRO parameter α such that the cluster probabilities P_γ are weighted throughout the calculation as follows:

$$P_{\mathrm{CuCu}} = P_{\mathrm{Cu}}P_{\mathrm{Cu}} + \alpha/4,$$

$$P_{\mathrm{CuZn}} = P_{\mathrm{Cu}}P_{\mathrm{Zn}} - \alpha/4,$$

$$P_{\mathrm{ZnCu}} = P_{\mathrm{Zn}}P_{\mathrm{Cu}} - \alpha/4,$$

$$P_{\mathrm{ZnZn}} = P_{\mathrm{Zn}}P_{\mathrm{Zn}} + \alpha/4.$$

Here $P_{Cu}=P_{Zn}=0.5$ and so α may take values in the range $-1<\alpha<+1$ where −1, 0, and +1 correspond to ideal ordering, complete randomness, and ideal clustering, respectively. Figures 2(d)–2(f) and Figs. 3(d)–3(f) show SCF-KKR-NLCPA calculations with $N_c=2$ for a selection of values of α decreasing from 0 to −1. For comparison, the corresponding (non-SCF) KKR-NLCPA results first given in Ref. 38 are shown in Figs. 2(a)–2(c) and Figs. 3(a)–3(c). As α decreases, the components of the total DOS due to like pairs decreases while that due to unlike pairs increases. The DOS has an increasing resemblance to that of the ordered $Cu_{50}Zn_{50}$ intermetallic compound (see the figure in Ref. 38) for both sets of results. Again differences are apparent between the non-SCF and SCF plots. In particular we see an increasing difference between the Cu−Cu and Cu−Zn components and between the Zn−Cu and Zn−Zn components for the SCF calculations as a result of charge transfer, and the bands are also closer together compared to the non-SCF calculations, further resembling the ordered calculation.

The fact that using the SCF-KKR-NLCPA means we now have two different Cu potentials and two different Zn potentials may be explicitly illustrated by demonstrating that there is a doubling of the core levels calculated using the conventional SCF-KKR-CPA. As an example, Fig. 4(a) shows that the 3*p* Cu core level is split into two levels at $\alpha=0$, each resulting from the fact that the Cu site now explicitly has either a Cu or a Zn neighbor. Similarly, Fig. 4(b) shows that the 3*p* Zn core level is split into two levels since the Zn site now explicitly has either a Cu or a Zn neighbor. Clearly, it would be of interest to observe such doubling of the core levels using photoelectron spectroscopy.[58] It is also interesting to observe that the 3*p* core levels are also influenced by SRO, as shown in the same figures.

Finally let us consider the effects of SRO on the total energy of the system.[30] Since $Cu_{50}Zn_{50}$ is known to order into an intermetallic compound of *B*2 symmetry at the transition temperature T_c, we would expect the total energy to be lower for negative values of α, corresponding to short-range ordering. Figure 4(c) shows SCF-KKR-NLCPA calculations with $N_c=2$ for the total energy plotted as a function of SRO. Reassuringly, it can be seen that the total energy is indeed lowered as α decreases. Furthermore, the relationship be-

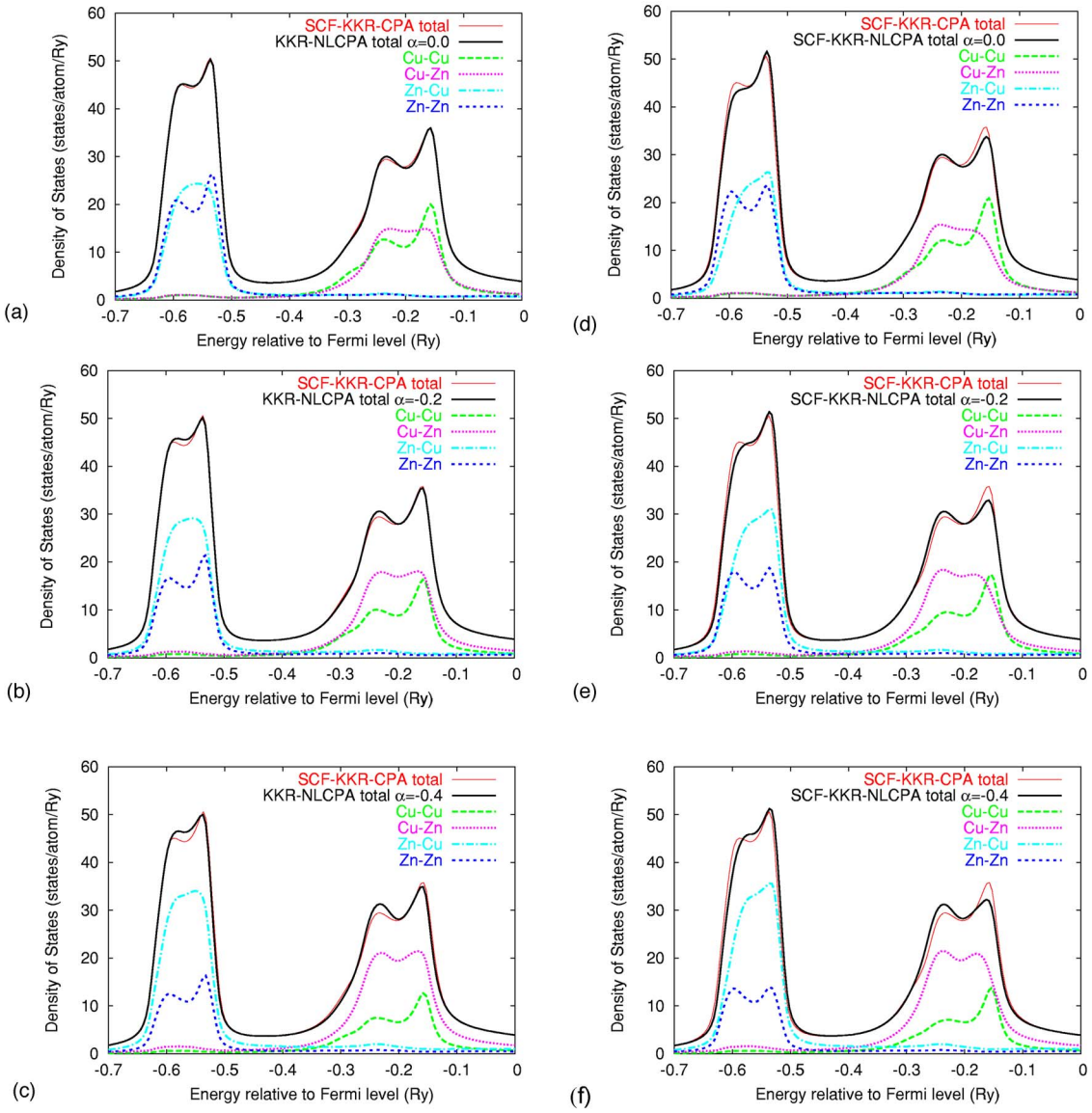

FIG. 2. (Color online) (a)–(c) KKR-NLCPA (non-SCF) $N_c=2$ DOS calculations for disordered bcc $Cu_{50}Zn_{50}$ with decreasing values of the SRO parameter α, corresponding to short-range ordering. (d)–(f) Same as (a)–(c) but using the new SCF-KKR-NLCPA.

tween the total energy and SRO parameter is shown in this case to be linear.

However, it should be stressed that the SCF-KKR-NLCPA is a theory of the electronic structure for a given ensemble of alloy configurations and is not a theory for what configurations actually occur in practice. For example, the extreme case corresponding to $\alpha=-1.0$ as defined above means that only unlike pairs are included in the $N_c=2$ cluster ensemble, a situation which would never occur in a real disordered alloy. Nevertheless, for the extreme case $\alpha=-1.0$, it can be seen that the total energy is lowered by 1.1 mRy, which would correspond to a lowering of T_c of roughly 250 K. This is useful as a crude order-of-magnitude estimate as to an upper bound on the possible lowering of T_c that could occur as a consequence of including nearest-neighbor SRO. The actual favored amount of SRO at a given temperature above T_c would need to be found by minimizing the corresponding free energy with respect to the SRO parameter α. This requires an expression for the configurational entropy term for the cluster with SRO (see Sec. IV).

B. $Cu_{60}Pd_{40}$ (fcc)

To test the ability of the SCF-KKR-NLCPA to capture the Madelung contribution to the total energy missing in the conventional SCF-KKR-CPA, we have studied the fcc $Cu_{60}Pd_{40}$ system, where the effect is expected to be larger than with the $Cu_{50}Zn_{50}$ system studied above. Figure 5(a) shows a SCF-KKR-NLCPA calculation with $N_c=4$ for the total DOS of the fcc $Cu_{60}Pd_{40}$ system, together with the conventional SCF-KKR-CPA results. The difference in the total DOS using the SCF-KKR-NLCPA compared to the SCF-KKR-CPA is shown in Fig. 5(b). We find that the Madelung contribution to the total energy calculated from Eq. (31) is −4.89 mRy. This is to be compared with the value of −6.8 mRy obtained in Ref. 57 using a large supercell calculation. Thus the SCF-

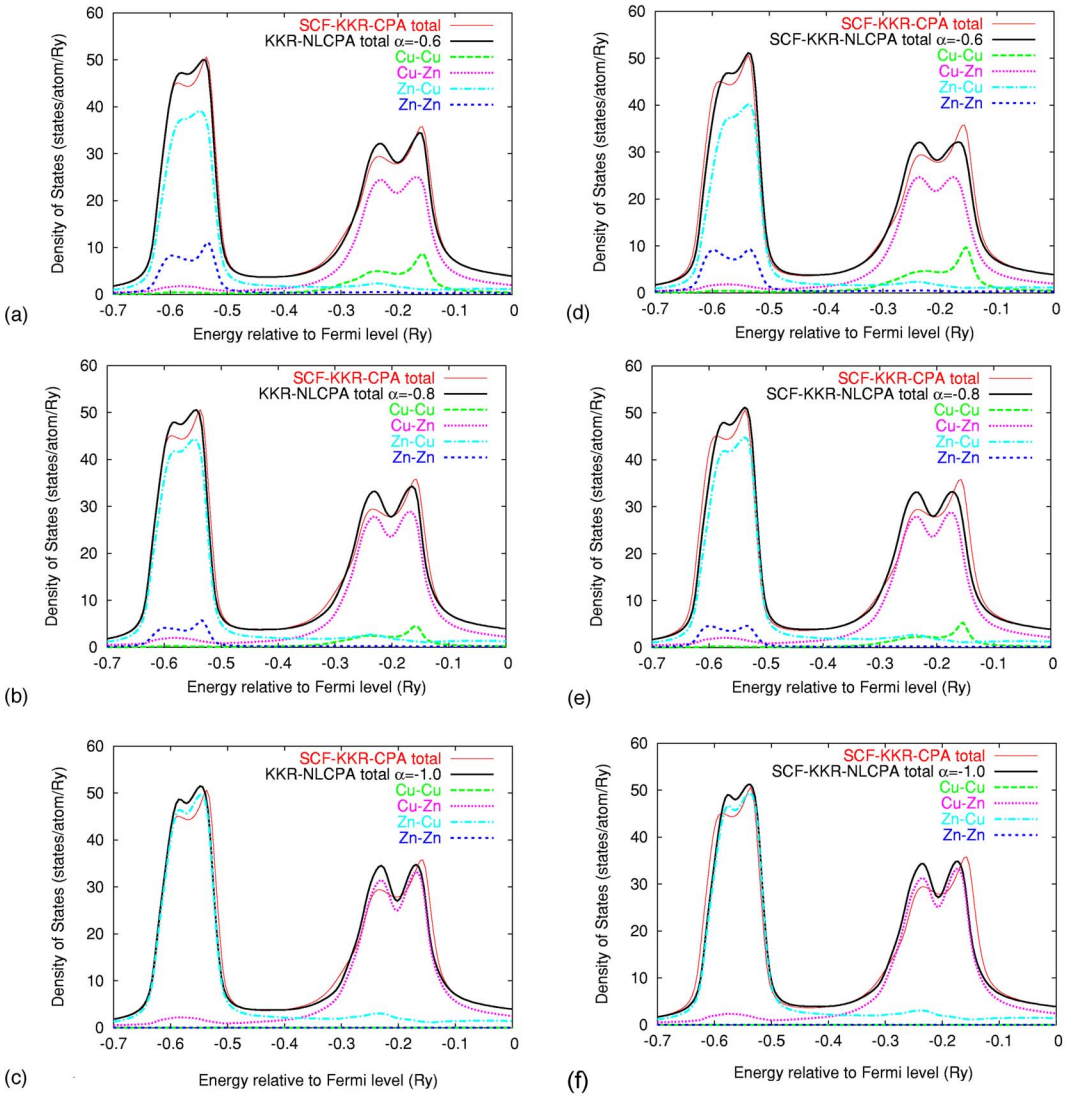

FIG. 3. (Color online) (a)–(c) Further KKR-NLCPA (non-SCF) $N_c=2$ DOS calculations for disordered bcc $Cu_{50}Zn_{50}$ with decreasing values of the SRO parameter α, corresponding to short-range ordering. (d)–(f) Same as (a)–(c) but using the new SCF-KKR-NLCPA.

KKR-NLCPA captures just over 2/3 of the Madelung energy for this system with $N_c=4$. However, it is clear that an investigation of the convergence of the theory with respect to cluster size should be carried out (see Sec. IV).

C. $Cu_{77}Ni_{23}$ (fcc)

To illustrate the effect of SRO on an fcc system, calculations are presented here for the much-studied $Cu_{77}Ni_{23}$ alloy.[23] First, Fig. 5(c) shows total DOS calculations using the SCF-KKR-NLCPA with $N_c=4$ and $\alpha=0$ (i.e., no SRO). While the difference in the total DOS compared to the conventional SCF-KKR-CPA result shown in the same figure is small, it is interesting to observe the component contributions to the total DOS from the 2^4 cluster configurations. Next we introduce the nearest-neighbor SRO parameter α such that the cluster probabilities P_γ are weighted throughout the calculation as follows:

$$P_{AAAA} = P_A P_A P_A P_A + C\alpha,$$

$$P_{AAAB} = P_{AABA} = P_{ABAA} = P_A P_A P_A P_B,$$

$$P_{AABB} = P_{ABAB} = P_{ABBA} = P_A P_A P_B P_B - C\alpha/3,$$

$$P_{ABBB} = P_A P_B P_B P_B,$$

$$P_{BAAA} = P_B P_A P_A P_A,$$

$$P_{BAAB} = P_{BABA} = P_{BBAA} = P_B P_A P_A P_B - C\alpha/3,$$

$$P_{BABB} = P_{BBAB} = P_{BBBA} = P_B P_A P_B P_B,$$

$$P_{BBBB} = P_B P_B P_B P_B + C\alpha,$$

where $C=3(P_A)^2(P_B)^2$ (here A=Cu and B=Ni). This means that α can take values in the range $-D \leqslant \alpha \leqslant +1$ where D is

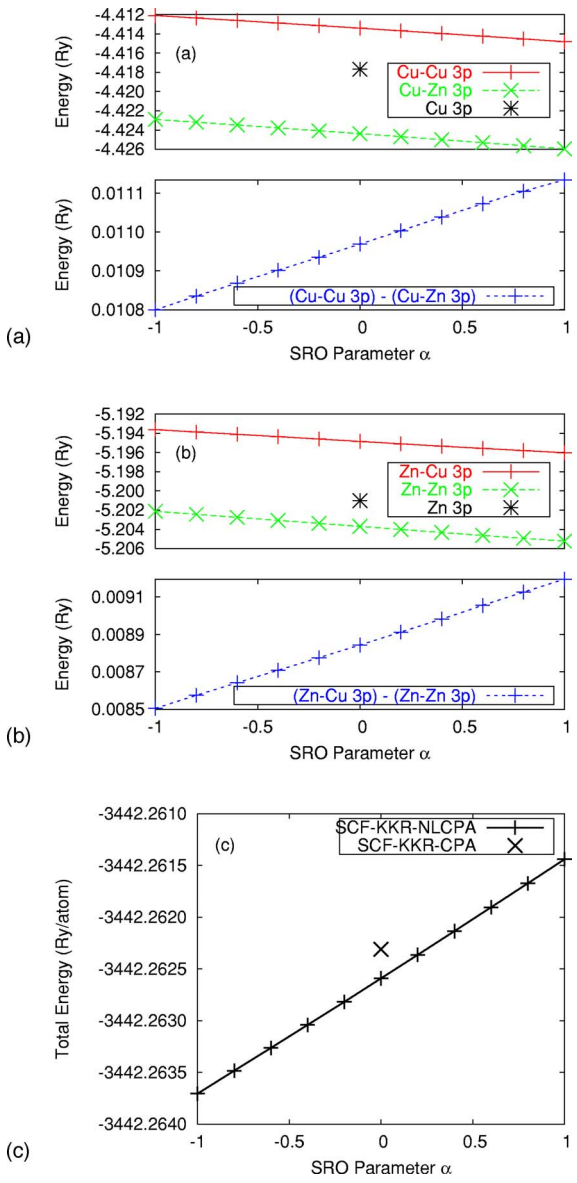

FIG. 4. (Color online) (a) SCF-KKR-NLCPA calculation for bcc $Cu_{50}Zn_{50}$ with $N_c=2$ showing the core $3p$ levels for the Cu–Cu and Cu–Zn components, plotted as a function of SRO. The lower figure shows the variation in the difference between the Cu–Cu and Cu–Zn components as a function of SRO. (b) Same as (a) but for the Zn–Cu and Zn–Zn components. (c) Plot of the total energy as a function of SRO for bcc $Cu_{50}Zn_{50}$ using the SCF-KKR-NLCPA with $N_c=2$. The conventional SCF-KKR-CPA result is also shown.

the smaller of $(P_A)^4/C$ and $(P_B)^4/C$. Negative values of α correspond to short-range ordering, and positive values of α correspond to short-range clustering. (The above distribution is based on the number of like and unlike pairs that exist for each cluster configuration. For example, components with three like and one unlike atoms are unaffected by SRO since the number of like and unlike pairs are equal in this case.) Since $Cu_{77}Ni_{23}$ is a clustering system, Fig. 5(d) shows the same SCF-KKR-NLCPA calculation as Fig. 5(c) but with $\alpha=+1.0$, corresponding to ideal short-range clustering. The difference in the total DOS between the SCF-KKR-NLCPA and SCF-KKR-CPA calculations has greatly increased. In particular the trough at approximately −0.1 Ry has deepened, as observed in photoemission expermients.[23] While the peak in the total DOS centered at approximately −0.05 Ry observed in photoemission experiments is not observed here, we do see its possible origin in the form of the all-Ni cluster component which has increased in magnitude and peaks at this energy.

IV. CONCLUSIONS

This paper has continued the development of the nonlocal KKR-CPA (KKR-NLCPA) method[36–38] for studying the electronic properties of disordered metallic alloys in the presence of SRO. Namely, a detailed description has been given and the first implementation reported of a fully self-consistent version of the procedure, which we refer to as the SCF-KKR-NLCPA. The power of the approach has been illustrated by explicit calculations for the $Cu_{50}Zn_{50}$, $Cu_{60}Pd_{40}$, and $Cu_{77}Ni_{23}$ systems.

The theory is unique and systematic since there are a unique set of allowed cluster sizes ranging from $N_c=1$ to $N_c=\infty$ for any given lattice. The SCF-KKR-NLCPA reduces to the conventional SCF-KKR-CPA for $N_c=1$ and becomes exact (within the LDA) as $N_c\rightarrow\infty$. In terms of computational cost, note that the SCF-KKR-NLCPA Brillouin zone integration does not scale as the cluster size increases, and like the conventional SCF-KKR-CPA, the integration may be carried out over the irreducible wedge corresponding to the chosen real-space tiling. For calculations with cluster sizes of $N_c=2$ and $N_c=4$ as presented here, there is therefore hardly any increase in computational cost over the conventional SCF-KKR-CPA method. Moreover, calculations with such cluster sizes are, for example, able to model the effects of nearest-neighbor SRO and are able to capture a large fraction of the Madelung energy for the systems studied here. However, calculations for larger cluster sizes will be computationally very demanding due to the 2^{N_c} real-space cluster configurations. Although the impurity cluster path matrices for each configuration are independent of each other and so the calculations could be run on parallel machines, it will clearly be necessary to use symmetry and importance sampling to greatly reduce the number of configurations. We intend to attempt such calculations and examine the convergence of the method with respect to cluster size in a future publication.

Finally, there is a fairly obvious general comment to be made with regard to the outlook for further progress based on the SCF-KKR-NLCPA. Clearly the cluster probabilities $\{P_\gamma\}$ used to calculate the total energy or electronic grand potential specify the corresponding cluster configurational entropy. These probabilities, which include a specification of SRO, may therefore be determined by constructing the appropriate free energy and minimizing it with respect to them. Evidently, such a procedure would amount to a fully first-principles cluster variational method[15] which can be expected to yield reliable alloy phase diagrams. Significantly, similar comments apply if, instead of concentration fluctuations as above, we are dealing with spin,[59] strain,[41] or valency fluctuations.[54]

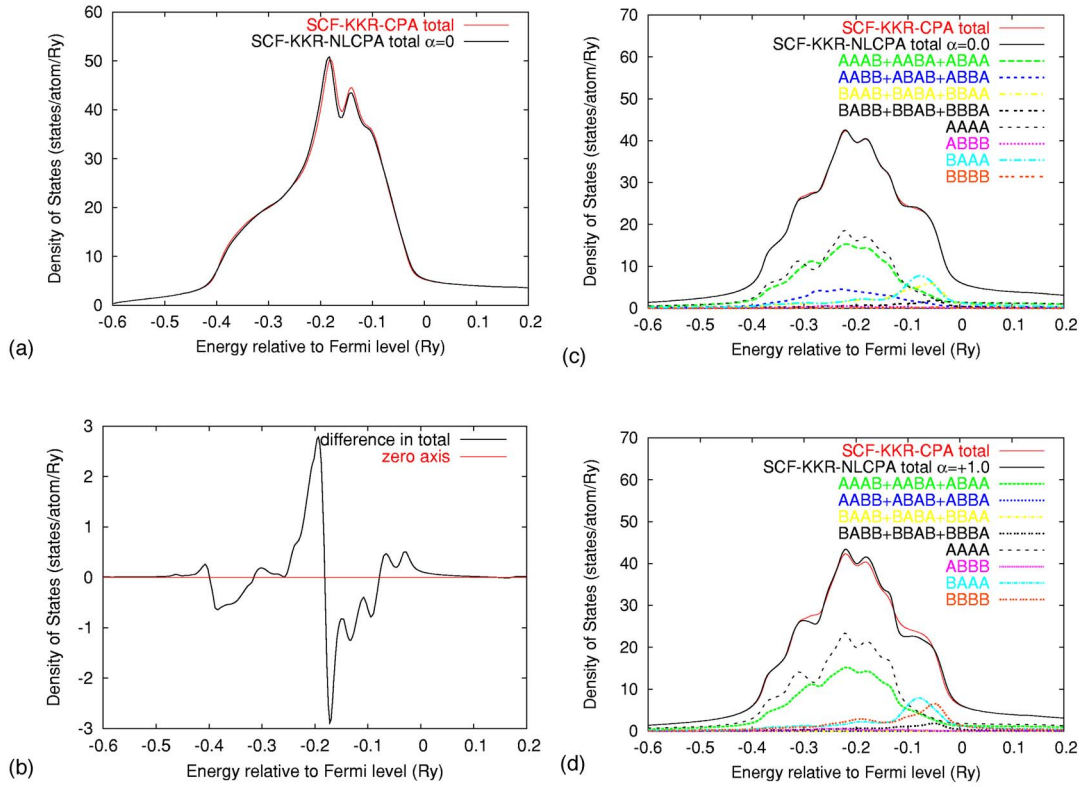

FIG. 5. (Color online) (a) SCF-KKR-NLCPA total DOS calculation with $N_c=4$ for fcc $Cu_{60}Pd_{40}$. Also shown are the non-SCF KKR-NLCPA and conventional SCF-KKR-CPA results. (b) Plot of the difference between the total SCF-KKR-NLCPA and SCF-KKR-CPA results shown in (a). (c) SCF-KKR-NLCPA total DOS calculation with $N_c=4$ for fcc $Cu_{77}Ni_{23}$ along with the component contributions from the 2^4 cluster configurations measured on the first labeled site. (Owing to translational invariance, measurement at any other cluster site would give the same results with a simple permutation of the labels.) Here A=Cu and B=Ni and components that are equivalent due to symmetry have been added together. The total SCF-KKR-CPA result is also shown. (d) Same as (c) but with $\alpha=+1.0$, corresponding to ideal short-range clustering.

ACKNOWLEDGMENT

D.A.R. acknowledges support from EPSRC (UK), Grant No. GR/S92212/01.

APPENDIX A: KKR-NLCPA LLOYD FORMULA—PROOF OF STATIONARITY

We begin from the expression for the KKR-NLCPA Lloyd formula, Eqs. (22) and (23). First, note that Eq. (23) can be rewritten in the form

$$\underline{\underline{\tau}}_{\gamma}^{-1} = \underline{\underline{t}}_{\gamma}^{-1} - \underline{\underline{\hat{t}}}^{-1} + \underline{\underline{\widehat{\delta G}}} + \underline{\underline{\hat{\tau}}}^{-1}, \tag{A1}$$

where $\underline{\underline{t}}_{\gamma}$ and $\underline{\underline{\hat{t}}}$ are diagonal in the cluster-site index. In other words, $\underline{\underline{t}}_{\gamma}$ is a supermatrix comprised of a cluster configuration γ of single-site scattering matrices $\underline{t}_{\alpha}$ along its diagonal, where α is the atomic species. Using the relation $\ln(\det \underline{\underline{A}}) = \mathrm{tr}_I \mathrm{tr}_L(\ln \underline{\underline{A}})$ where $\underline{\underline{A}}$ is a supermatrix in the cluster-site and angular momentum index, Eq. (22) may be rewritten as

$$\bar{N}(E) = \bar{N}_1 + \bar{N}_2, \tag{A2}$$

where

$$\bar{N}_1 = N_0(E) - \frac{1}{\pi}\frac{1}{\Omega_{BZ}} \mathrm{Im} \sum_{\mathbf{K}_n} \int_{\Omega_{\mathbf{K}_n}} d\mathbf{k}\, \mathrm{tr}_L \times \ln[\underline{\hat{t}}^{-1} - \underline{\widehat{\delta G}}(\mathbf{K}_n) - \underline{G}(\mathbf{k})] \tag{A3}$$

and

$$\bar{N}_2 = -\frac{1}{\pi N_c} \mathrm{Im} \sum_{\gamma} P_{\gamma}\, \mathrm{tr}_I\, \mathrm{tr}_L(\ln \underline{\underline{\tau}}_{\gamma}^{-1} - \ln \underline{\underline{\hat{\tau}}}^{-1}). \tag{A4}$$

First let us consider the variation with respect to the effective inverse cluster t matrix $\underline{\hat{t}}^{-1}$. Now,

$$\frac{\delta(\bar{N}_1)}{\delta \underline{\hat{t}}^{-1}} = -\frac{1}{\pi}\frac{1}{\Omega_{BZ}} \mathrm{Im} \sum_{\mathbf{K}_n} \int_{\Omega_{\mathbf{K}_n}} d\mathbf{k}\, \mathrm{tr}_L [\underline{\hat{t}}^{-1} - \underline{\widehat{\delta G}}(\mathbf{K}_n) - \underline{G}(\mathbf{k})]^{-1}$$

$$= -\frac{1}{\pi} \mathrm{Im}\, \mathrm{tr}_L \frac{1}{N_c} \sum_{\mathbf{K}_n} \underline{\hat{\tau}}(\mathbf{K}_n)$$

$$= -\frac{1}{\pi} \mathrm{Im}\, \mathrm{tr}_L\, \underline{\hat{\tau}}^{II}$$

$$= -\frac{1}{\pi N_c}\,\mathrm{Im}\,\mathrm{tr}_I\,\mathrm{tr}_L\hat{\underline{\underline{\tau}}}, \tag{A5}$$

since $\hat{\underline{\underline{\tau}}}$ is a translationally invariant quantity. Also,

$$\begin{aligned}\frac{\delta(\bar{N}_2)}{\delta\hat{\underline{t}}^{-1}} &= -\frac{1}{\pi N_c}\,\mathrm{Im}\sum_\gamma P_\gamma\,\mathrm{tr}_I\,\mathrm{tr}_L\left(\underline{\underline{\tau}}_\gamma\frac{\delta}{\delta\hat{\underline{t}}^{-1}}(\underline{\underline{\tau}}_\gamma^{-1}) - \hat{\underline{\underline{\tau}}}\frac{\delta}{\delta\hat{\underline{t}}^{-1}}(\hat{\underline{\underline{\tau}}})\right)\\ &= -\frac{1}{\pi N_c}\,\mathrm{Im}\sum_\gamma P_\gamma\,\mathrm{tr}_I\,\mathrm{tr}_L\left(\underline{\underline{\tau}}_\gamma\frac{\delta}{\delta\hat{\underline{t}}^{-1}}(\underline{\underline{t}}_\gamma^{-1} - \hat{\underline{\underline{t}}}^{-1}\right.\\ &\quad\left. + \widehat{\underline{\underline{\underline{\underline{\delta G}}}}} + \hat{\underline{\underline{\tau}}} - \hat{\underline{\underline{\tau}}})\right)\\ &= -\frac{1}{\pi N_c}\,\mathrm{Im}\sum_\gamma P_\gamma\,\mathrm{tr}_I\,\mathrm{tr}_L(-\underline{\underline{\tau}}_\gamma)\\ &= +\frac{1}{\pi N_c}\,\mathrm{Im}\,\mathrm{tr}_I\,\mathrm{tr}_L\hat{\underline{\underline{\tau}}}.\end{aligned} \tag{A6}$$

By adding Eqs. (A5) and (A6) we arrive at the result

$$\frac{\delta\bar{N}(E)}{\delta\hat{\underline{t}}^{-1}} = 0; \tag{A7}$$

i.e., $\bar{N}(E)$ is stationary with respect to the effective inverse cluster t matrix.

Now let us consider the variation of $\bar{N}(E)$ with respect to the effective structure constant corrections $\widehat{\underline{\delta G}}(\mathbf{K}_n)$. Using the same argument as that given in Eq. (A5) we get

$$\frac{\delta(\bar{N}_1)}{\widehat{\underline{\delta G}}(\mathbf{K}_n)} = +\frac{1}{\pi N_c}\,\mathrm{Im}\,\mathrm{tr}_I\,\mathrm{tr}_L\hat{\underline{\underline{\tau}}}. \tag{A8}$$

Also,

$$\begin{aligned}\frac{\delta(\bar{N}_2)}{\widehat{\underline{\delta G}}(\mathbf{K}_n)} &= -\frac{1}{\pi N_c}\,\mathrm{Im}\sum_\gamma P_\gamma\,\mathrm{tr}_I\,\mathrm{tr}_L\left(\underline{\underline{\tau}}_\gamma\frac{\delta}{\widehat{\underline{\delta G}}(\mathbf{K}_n)}(\underline{\underline{t}}_\gamma^{-1} - \hat{\underline{\underline{t}}}^{-1}\right.\\ &\quad\left. + \widehat{\underline{\underline{\underline{\underline{\delta G}}}}} + \hat{\underline{\underline{\tau}}} - \hat{\underline{\underline{\tau}}})\right)\\ &= -\frac{1}{\pi N_c}\,\mathrm{Im}\sum_\gamma P_\gamma\,\mathrm{tr}_I\,\mathrm{tr}_L(\underline{\underline{\tau}}_\gamma)\\ &= -\frac{1}{\pi N_c}\,\mathrm{Im}\,\mathrm{tr}_I\,\mathrm{tr}_L\hat{\underline{\underline{\tau}}},\end{aligned} \tag{A9}$$

where Eq. (4) has been used. Finally, by adding Eqs. (A8) and (A9) we arrive at the result

$$\frac{\delta\bar{N}(E)}{\widehat{\underline{\delta G}}(\mathbf{K}_n)} = 0; \tag{A10}$$

i.e., $\bar{N}(E)$ is stationary with respect to the effective structure constant corrections in reciprocal space. The same is true in real space from Eq. (4).

APPENDIX B: DERIVATION OF $\delta N/\delta\mu$

We begin from the expression for the KKR-NLCPA Lloyd formula, Eqs. (22) and (23). Rewriting Eq. (23) in the form of Eq. (A1), let us introduce notation such that

$$[\hat{\underline{t}}^{-1}]^I_{LL'} = [\underline{\underline{\hat{m}}}]^I_{LL'} = \hat{m}^I_{LL'},$$

$$[\underline{t}_\gamma^{-1}]^I_{LL'} = [\underline{\underline{m}}_\gamma]^I_{LL'} = m^I_{\gamma LL'}.$$

As a generalization of the argument of Appendix B of Ref. 9, $\bar{N}(E,\mu)$ now depends on μ only through the matrices $\underline{\underline{m}}_\gamma$, $\underline{\underline{\hat{m}}}$, $\widehat{\underline{\underline{\underline{\underline{\delta G}}}}}$, and $\underline{\delta G}(\mathbf{K}_n)$. From the chain rule it follows that

$$\begin{aligned}\frac{\delta\bar{N}}{\delta\mu'} &= \sum_{LL'}\sum_{K_n}\left[\frac{\delta\bar{N}}{\delta(\delta G_{LL'}(\mathbf{K}_n))}\frac{\delta(\delta G_{LL'}(\mathbf{K}_n))}{\delta\mu'}\right]\\ &\quad+\sum_{LL'}\sum_{IJ}\left[\frac{\delta\bar{N}}{\delta\hat{m}^I_{LL'}}\frac{\delta\hat{m}^I_{LL'}}{\delta\mu'} + \frac{\delta\bar{N}}{\delta(\widehat{\delta G}^{IJ}_{LL'})}\frac{\delta(\widehat{\delta G}^{IJ}_{LL'})}{\delta\mu'}\right.\\ &\quad\left.+\sum_\gamma\frac{\delta\bar{N}}{\delta m^I_{\gamma LL'}}\frac{\delta m^I_{\gamma LL'}}{\delta\mu'}\right].\end{aligned} \tag{B1}$$

However, since $\bar{N}$ is stationary with respect to both variations in the effective t matrices and effective structure constant corrections (see Appendix A), only the final term in Eq. (B1) remains—i.e.,

$$\frac{\delta\bar{N}}{\delta\mu'} = \sum_{LL'}\sum_I\sum_\gamma\frac{\delta\bar{N}}{\delta m^I_{\gamma LL'}}\frac{\delta m^I_{\gamma LL'}}{\delta\mu'}. \tag{B2}$$

Now by using the chain rule we have

$$\frac{\delta\underline{\underline{m}}^I_\gamma}{\delta\mu'} = \int d\mathbf{r}_I\frac{\delta\underline{\underline{m}}^I_\gamma}{\delta v_\gamma(\mathbf{r}_I)}\frac{\delta v_\gamma(\mathbf{r}_I)}{\delta\mu'} \tag{B3}$$

and so

$$\frac{\delta\bar{N}}{\delta\mu'} = \sum_{LL'}\sum_I\sum_\gamma\frac{\delta\bar{N}}{\delta m^I_{\gamma LL'}}\left(\int d\mathbf{r}_I\frac{\delta m^I_{\gamma LL'}}{\delta v_\gamma(\mathbf{r}_I)}\frac{\delta v_\gamma(\mathbf{r}_I)}{\delta\mu'}\right). \tag{B4}$$

Note that the variation of the single-site scattering matrices with respect to arbitrary, not just spherically symmetric, changes in the local potential at a site i is given by[60]

$$\frac{\delta m^i_{\alpha LL'}}{\delta v_\alpha(\mathbf{r}_i)} = -Z_{\alpha,L}(\mathbf{r}_i,E)Z_{\alpha,L'}(\mathbf{r}_i,E), \tag{B5}$$

where $Z_{\alpha,L}(\mathbf{r}_i,E)$ is the regular solution of the Schrödinger equation at energy E and α is the atomic species. Now using the above relation, it is clear that

$$\frac{\delta m^I_{\gamma LL'}}{\delta v_\gamma(\mathbf{r}_I)} = -Z_{\gamma,L}(\mathbf{r}_I,E)Z_{\gamma,L'}(\mathbf{r}_I,E) \tag{B6}$$

for each cluster site I, where $\underline{Z}_\gamma(\mathbf{r}_I,E)$ has been defined in Sec. II B.

Next, using the expression for $\bar{N}$ given by the Lloyd formula, Eq. (22), and the relation $\ln(\det\underline{\underline{A}}) = \mathrm{tr}_I\,\mathrm{tr}_L(\ln\underline{\underline{A}})$ where

$\underline{\underline{A}}$ is a supermatrix in the cluster-site and angular momentum index, we obtain

$$\frac{\delta \bar{N}}{\delta \underline{m}_\gamma^I} = -\frac{1}{\pi N_c} P_\gamma \,\mathrm{Im}\, \underline{\tau}_\gamma^{II} \tag{B7}$$

for each cluster site I. Inserting Eqs. (B6) and (B7) into Eq. (B4) gives

$$\frac{\delta \bar{N}}{\delta \mu'} = \frac{1}{\pi N_c} \sum_I \sum_{LL'} \sum_\gamma P_\gamma \int d\mathbf{r}_I \frac{\delta v_\gamma(\mathbf{r}_I)}{\delta \mu'} \mathrm{Im}\, Z_{\gamma,L}(\mathbf{r}_I, E) \times \tau_{\gamma LL'}^{II} Z_{\gamma,L'}(\mathbf{r}_I, E). \tag{B8}$$

This may be rewritten as

$$\frac{\delta \bar{N}}{\delta \mu'} = \frac{1}{\pi N_c} \sum_I \sum_{LL'} \sum_\gamma P_\gamma \int d\mathbf{r}_I \,\mathrm{Im}\, G_{\gamma,LL'}(\mathbf{r}_I, \mathbf{r}_I, E) \frac{\delta v_\gamma(\mathbf{r}_I)}{\delta \mu'}, \tag{B9}$$

where the impurity cluster Green's function matrix elements are defined by Eq. (16). Equation (21) now becomes

$$\bar{\Omega} = \mu \bar{N}(\mu, \mu) - \int_{-\infty}^{\mu} dE \bar{N}(E, \mu) + \frac{1}{N_c} \int_{-\infty}^{\mu} d\mu' \sum_\gamma P_\gamma \,\mathrm{Im} \sum_I \sum_{LL'} \times \frac{1}{\pi} \int_{-\infty}^{\mu'} dE \int d\mathbf{r}_I [\underline{G}_\gamma(\mathbf{r}_I, \mathbf{r}_I, E)]_{LL'} \frac{\delta v_\gamma(\mathbf{r}_I, \mu')}{\delta \mu'}. \tag{B10}$$

Using the definition of the cluster component charge density matrix elements given by Eq. (18), Eq. (B10) can be rewritten as Eq. (24) given in Sec. II E.

APPENDIX C: ELECTRONIC GRAND POTENTIAL FROM THE CHOSEN LOCAL POTENTIAL

It is straightforward to derive Eq. (29) from Eqs. (25) and (26). As an example consider the first term in Eq. (26), which corresponds to the fourth term in Eq. (29)—i.e.,

$$v_\gamma^{(1)}(\mathbf{r}_I) = \sum_J \int d\mathbf{r}_J' \frac{\rho_\gamma(\mathbf{r}_J')}{|\mathbf{r}_I - \mathbf{r}_J' + \mathbf{R}_{IJ}|}. \tag{C1}$$

Inserting into the final term of Eq. (25) gives

$$\bar{\Omega}^{(4)} = \frac{1}{N_c} \int_{-\infty}^{\mu} d\mu' \sum_\gamma P_\gamma \sum_{I,J} \frac{\int d\mathbf{r}_I (d\rho_\gamma(\mathbf{r}_I, \mu')/d\mu') \int d\mathbf{r}_J' \rho_\gamma(\mathbf{r}_J', \mu')}{|\mathbf{r}_I - \mathbf{r}_J' + \mathbf{R}_{IJ}|} = \frac{1}{N_c} \sum_\gamma P_\gamma \sum_{I,J} \frac{\int d\mathbf{r}_I \rho_\gamma(\mathbf{r}_I, \mu) \int d\mathbf{r}_J' \rho_\gamma(\mathbf{r}_J', \mu)}{|\mathbf{r}_I - \mathbf{r}_J' + \mathbf{R}_{IJ}|} - \bar{\Omega}^{(4)}. \tag{C2}$$

Therefore

$$\bar{\Omega}^{(4)} = \frac{1}{2} \frac{1}{N_c} \sum_\gamma P_\gamma \sum_{I,J} \frac{\int d\mathbf{r}_I \rho_\gamma(\mathbf{r}_I, \mu) \int d\mathbf{r}_J' \rho_\gamma(\mathbf{r}_J', \mu)}{|\mathbf{r}_I - \mathbf{r}_J' + \mathbf{R}_{IJ}|}, \tag{C3}$$

as seen in Eq. (29). The remaining terms follow similarly.

APPENDIX D: ELECTRONIC GRAND POTENTIAL—PROOF OF STATIONARITY

The aim is to show that $\delta(\Omega - \mu \bar{N}) / \delta(\rho_\gamma(\mathbf{r}_I)) = 0$ for each cluster configuration γ where $\mathbf{r}_I$ is a point within any cluster site I. First let us consider the variation of the kinetic part of Ω. Now,

$$\frac{\delta(T - \mu \bar{N})}{\delta \rho_\gamma(\mathbf{r}_I)} = T_1 + T_2, \tag{D1}$$

where

$$T_1 = -\int_{-\infty}^{\mu} dE \frac{\delta \bar{N}(E, \mu)}{\delta \rho_\gamma(\mathbf{r}_I)} \tag{D2}$$

and

$$T_2 = -\frac{1}{N_c} \sum_{\gamma'} P_{\gamma'} \sum_J \int d\mathbf{r}_J' \frac{\delta}{\delta \rho_\gamma(\mathbf{r}_I)} [\rho_{\gamma'}(\mathbf{r}_J') v_{\gamma'}(\mathbf{r}_J')]. \tag{D3}$$

First consider T_1. By using the chain rule and the notation introduced in Appendix B we have

$$T_1 = -\int_{-\infty}^{\mu} dE \sum_{\gamma'} \sum_{LL'} \sum_J \int d\mathbf{r}_J' \frac{\delta \bar{N}}{\delta m_{\gamma' LL'}^J} \frac{\delta m_{\gamma' LL'}^J}{\delta v_{\gamma'}(\mathbf{r}_J')} \frac{\delta v_{\gamma'}(\mathbf{r}_J')}{\delta \rho_\gamma(\mathbf{r}_I)}. \tag{D4}$$

By using Eqs. (B6) and (B7) and the definition of the cluster component charge density, Eq. (18), we arrive at

$$T_1 = +\frac{1}{N_c} \sum_{\gamma'} P_{\gamma'} \sum_J \int d\mathbf{r}_J' \rho_{\gamma'}(\mathbf{r}_J') \frac{\delta v_{\gamma'}(\mathbf{r}_J')}{\delta \rho_\gamma(\mathbf{r}_I)}. \tag{D5}$$

Now consider T_2. Using the product rule we have

$$T_2 = -\frac{1}{N_c}\sum_{\gamma'} P_{\gamma'} \sum_J \int d\mathbf{r}'_J \times \left(\rho_{\gamma'}(\mathbf{r}'_J)\frac{\delta v_{\gamma'}(\mathbf{r}'_J)}{\delta \rho_\gamma(\mathbf{r}_I)} + v_{\gamma'}(\mathbf{r}'_J)\frac{\delta \rho_{\gamma'}(\mathbf{r}'_J)}{\delta \rho_\gamma(\mathbf{r}_I)} \right), \tag{D6}$$

and so

$$T_2 = -\frac{1}{N_c}\sum_{\gamma'} P_{\gamma'} \sum_J \int d\mathbf{r}'_J \rho_{\gamma'}(\mathbf{r}'_J)\frac{\delta v_{\gamma'}(\mathbf{r}'_J)}{\delta \rho_\gamma(\mathbf{r}_I)} - \frac{1}{N_c} P_\gamma v_\gamma(\mathbf{r}_I) \tag{D7}$$

using the properties of functional differentiation. By adding T_1 and T_2 we get

$$\frac{\delta(T-\mu\bar{N})}{\delta \rho_\gamma(\mathbf{r}_I)} = -\frac{1}{N_c} P_\gamma v_\gamma(\mathbf{r}_I) \tag{D8}$$

for $\mathbf{r}$ within any cluster site I.

Next, consider the variation of U, the remaining terms in Eq. (29). As an example consider Eq. (C3), the fourth term of Ω. We have

$$\begin{aligned}
\frac{\delta \bar{\Omega}^{(4)}}{\delta \rho_\gamma(\mathbf{r}_I)} &= \frac{1}{2}\frac{1}{N_c}\sum_{\gamma'} P_{\gamma'} \sum_{J,K} \left[\frac{\int d\mathbf{r}'_J \rho_{\gamma'}(\mathbf{r}'_J)}{|\mathbf{r}'_J - \mathbf{r}''_K + \mathbf{R}_{JK}|} \int d\mathbf{r}''_K \frac{\delta \rho_{\gamma'}(\mathbf{r}''_K)}{\delta \rho_\gamma(\mathbf{r}_I)} \right. \\
&\quad \left. + \int d\mathbf{r}'_J \frac{\delta \rho_{\gamma'}(\mathbf{r}'_J)}{\delta \rho_\gamma(\mathbf{r}_I)} \frac{\int d\mathbf{r}''_K \rho_{\gamma'}(\mathbf{r}''_K)}{|\mathbf{r}'_J - \mathbf{r}''_K + \mathbf{R}_{JK}|} \right] \\
&= \frac{1}{2}\frac{1}{N_c} P_\gamma \left[\sum_J \frac{\int d\mathbf{r}'_J \rho_\gamma(\mathbf{r}'_J)}{|\mathbf{r}'_J - \mathbf{r}_I + \mathbf{R}_{JI}|} + \sum_K \frac{\int d\mathbf{r}''_K \rho_\gamma(\mathbf{r}''_K)}{|\mathbf{r}_I - \mathbf{r}''_K + \mathbf{R}_{IK}|} \right] \\
&= \frac{1}{N_c} P_\gamma \sum_J \int d\mathbf{r}'_J \frac{\rho_\gamma(\mathbf{r}'_J)}{|\mathbf{r}_I - \mathbf{r}'_J + \mathbf{R}_{IJ}|} \\
&= +\frac{1}{N_c} P_\gamma v_\gamma^{(1)}(\mathbf{r}_I),
\end{aligned} \tag{D9}$$

i.e., the first term in Eq. (26). The remaining terms follow similarly, leading to

$$\frac{\delta(U)}{\delta \rho_\gamma(\mathbf{r}_I)} = +\frac{1}{N_c} P_\gamma v_\gamma(\mathbf{r}_I) \tag{D10}$$

for $\mathbf{r}$ within any cluster site I. Finally, by adding Eqs. (D8) and (D10), we have proved that

$$\frac{\delta(\Omega - \mu\bar{N})}{\delta(\rho_\gamma(\mathbf{r}_I))} = 0 \tag{D11}$$

for each cluster configuration γ where $\mathbf{r}_I$ is a point within any cluster site I.

APPENDIX E: TRANSLATIONAL INVARIANCE

Due to the single-site translational invariance of the KKR-NLCPA effective medium, every site in the cluster experiences the same environment after averaging over all cluster configurations. This means that, in practice, calculating the total energy via Eq. (29) would amount to performing the same calculation N_c times and then dividing by N_c. Clearly, the total energy expression (29) can be simplified by removing the $1/N_c$ factor and the sum over the cluster site index I, although the sum over J remains. In other words, although cluster-restricted-average quantities are always dealt with, in practice the potential matrix $\underline{v}_\gamma(\mathbf{r})$ only needs to be considered with $\mathbf{r}$ restricted to lie within a general reference site I—i.e., $\mathbf{r}_I$—in Eq. (29) when calculating the electronic grand potential. Of course, it does not matter which site is chosen to be site I since all sites are equivalent on the average. For computational purposes Eq. (29) may therefore be rewritten in the simplified form

$$\begin{aligned}
\Omega &= \mu\bar{N}(\mu,\mu) - \int_{-\infty}^{\mu} dE \bar{N}(E,\mu) \\
&\quad - \sum_\gamma P_\gamma \int d\mathbf{r}_I \rho_\gamma(\mathbf{r}_I,\mu) v_\gamma(\mathbf{r}_I,\mu) \\
&\quad + \frac{1}{2}\sum_\gamma P_\gamma \sum_J \frac{\int d\mathbf{r}_I \rho_\gamma(\mathbf{r}_I) \int d\mathbf{r}'_J \rho_\gamma(\mathbf{r}'_J)}{|\mathbf{r}_I - \mathbf{r}'_J + \mathbf{R}_{IJ}|} \\
&\quad + \sum_\gamma P_\gamma \sum_J \frac{\int d\mathbf{r}_I \rho_\gamma(\mathbf{r}_I) Z_\gamma^J}{|\mathbf{r}_I + \mathbf{R}_{IJ}|} \\
&\quad + \frac{1}{2}\sum_\gamma P_\gamma \sum_{n \notin C} \frac{\int d\mathbf{r}_I \rho_\gamma(\mathbf{r}_I) \int d\mathbf{r}'_n \bar{\rho}(\mathbf{r}'_n)}{|\mathbf{r}_I - \mathbf{r}'_n + \mathbf{R}_{In}|} \\
&\quad + \sum_\gamma P_\gamma \sum_{n \notin C} \frac{\int d\mathbf{r}_I \rho_\gamma(\mathbf{r}_I) \bar{Z}^n}{|\mathbf{r}_I + \mathbf{R}_{In}|} \\
&\quad + \sum_\gamma P_\gamma \int d\mathbf{r}_I \rho_\gamma(\mathbf{r}_I) v_\gamma^{xc}[\rho_\gamma(\mathbf{r}_I)].
\end{aligned} \tag{E1}$$

The Madelung contribution to the total energy per site, Eq. (31), becomes

$$E_M = \frac{1}{2}\sum_\gamma P_\gamma \sum_{J \neq I} \frac{\int d\mathbf{r}_I \rho_\gamma(\mathbf{r}_I)[\int d\mathbf{r}'_J \rho_\gamma(\mathbf{r}'_J) - 2Z_\gamma^J]}{|\mathbf{r}_I - \mathbf{r}'_J + \mathbf{R}_{IJ}|}. \tag{E2}$$

APPENDIX F: CHARGE SELF-CONSISTENCY EXAMPLE—BINARY ALLOY WITH $N_c = 2$

(i) Begin with an appropriate guess for the cluster potential matrices $\underline{v}_{AA}(\mathbf{r})$, $\underline{v}_{AB}(\mathbf{r})$, $\underline{v}_{BA}(\mathbf{r})$, and $\underline{v}_{BB}(\mathbf{r})$, where

$$\underline{v}_{AA}(\mathbf{r}) = \begin{bmatrix} v_{AA}(\mathbf{r}_I) & 0 \\ 0 & v_{AA}(\mathbf{r}_J) \end{bmatrix},$$

$$\underline{v}_{AB}(\mathbf{r}) = \begin{bmatrix} v_{AB}(\mathbf{r}_I) & 0 \\ 0 & v_{AB}(\mathbf{r}_J) \end{bmatrix},$$

$$\underline{v}_{BA}(\mathbf{r}) = \begin{bmatrix} v_{BA}(\mathbf{r}_I) & 0 \\ 0 & v_{BA}(\mathbf{r}_J) \end{bmatrix},$$

$$\underline{v}_{BB}(\mathbf{r}) = \begin{bmatrix} v_{BB}(\mathbf{r}_I) & 0 \\ 0 & v_{BB}(\mathbf{r}_J) \end{bmatrix}.$$

An appropriate first guess could be to use the CPA potentials; e.g., for $\gamma=AB$ let $v_{AB}(\mathbf{r}_I)=v_A(\mathbf{r}_I)$ and $v_{AB}(\mathbf{r}_J)=v_B(\mathbf{r}_J)$.

(ii) Determine the effective medium using the KKR-NLCPA and calculate the site-diagonal part of the impurity cluster Green's functions:

$$\underline{\underline{G}}_{AA}(\mathbf{r},\mathbf{r},E) = \begin{bmatrix} \underline{Z}_A(\mathbf{r}_I)\underline{\tau}_{AA}^{JI}\underline{Z}_A(\mathbf{r}_I) - \underline{Z}_A(\mathbf{r}_I)\underline{J}_A(\mathbf{r}_I) & 0 \\ 0 & \underline{Z}_A(\mathbf{r}_J)\underline{\tau}_{AA}^{JJ}\underline{Z}_A(\mathbf{r}_J) - \underline{Z}_A(\mathbf{r}_J)\underline{J}_A(\mathbf{r}_J) \end{bmatrix},$$

$$\underline{\underline{G}}_{AB}(\mathbf{r},\mathbf{r},E) = \begin{bmatrix} \underline{Z}_A(\mathbf{r}_I)\underline{\tau}_{AB}^{JI}\underline{Z}_A(\mathbf{r}_I) - \underline{Z}_A(\mathbf{r}_I)\underline{J}_A(\mathbf{r}_I) & 0 \\ 0 & \underline{Z}_B(\mathbf{r}_J)\underline{\tau}_{AB}^{JJ}\underline{Z}_B(\mathbf{r}_J) - \underline{Z}_B(\mathbf{r}_J)\underline{J}_B(\mathbf{r}_J) \end{bmatrix},$$

$$\underline{\underline{G}}_{BA}(\mathbf{r},\mathbf{r},E) = \begin{bmatrix} \underline{Z}_B(\mathbf{r}_I)\underline{\tau}_{BA}^{JI}\underline{Z}_B(\mathbf{r}_I) - \underline{Z}_B(\mathbf{r}_I)\underline{J}_B(\mathbf{r}_I) & 0 \\ 0 & \underline{Z}_A(\mathbf{r}_J)\underline{\tau}_{BA}^{JJ}\underline{Z}_A(\mathbf{r}_J) - \underline{Z}_A(\mathbf{r}_J)\underline{J}_A(\mathbf{r}_J) \end{bmatrix},$$

$$\underline{\underline{G}}_{BB}(\mathbf{r},\mathbf{r},E) = \begin{bmatrix} \underline{Z}_B(\mathbf{r}_I)\underline{\tau}_{BB}^{JI}\underline{Z}_B(\mathbf{r}_I) - \underline{Z}_B(\mathbf{r}_I)\underline{J}_B(\mathbf{r}_I) & 0 \\ 0 & \underline{Z}_B(\mathbf{r}_J)\underline{\tau}_{BB}^{JJ}\underline{Z}_B(\mathbf{r}_J) - \underline{Z}_B(\mathbf{r}_J)\underline{J}_B(\mathbf{r}_J) \end{bmatrix}.$$

(iii) Using the above, calculate the corresponding cluster component charge densities:

$$\underline{\rho}_{AA}(\mathbf{r}) = \begin{bmatrix} \rho_{AA}(\mathbf{r}_I) & 0 \\ 0 & \rho_{AA}(\mathbf{r}_J) \end{bmatrix},$$

$$\underline{\rho}_{AB}(\mathbf{r}) = \begin{bmatrix} \rho_{AB}(\mathbf{r}_I) & 0 \\ 0 & \rho_{AB}(\mathbf{r}_J) \end{bmatrix},$$

$$\underline{\rho}_{BA}(\mathbf{r}) = \begin{bmatrix} \rho_{BA}(\mathbf{r}_I) & 0 \\ 0 & \rho_{BA}(\mathbf{r}_J) \end{bmatrix},$$

$$\underline{\rho}_{BB}(\mathbf{r}) = \begin{bmatrix} \rho_{BB}(\mathbf{r}_I) & 0 \\ 0 & \rho_{BB}(\mathbf{r}_J) \end{bmatrix}.$$

(iv) Reconstruct new cluster potentials. As an example, for $\underline{v}_{AB}(\mathbf{r})$ the matrix elements are given by

$$v_{AB}(\mathbf{r}_I) = \frac{\int d\mathbf{r}'_I \rho_{AB}(\mathbf{r}'_I)}{|\mathbf{r}_I - \mathbf{r}'_I|} + \frac{\int d\mathbf{r}'_J \rho_{AB}(\mathbf{r}'_J)}{|\mathbf{r}_I - \mathbf{r}'_J + \mathbf{R}_{IJ}|} + \frac{Z_{AB}^I}{|\mathbf{r}_I|} + \frac{Z_{AB}^J}{|\mathbf{r}_I + \mathbf{R}_{IJ}|} + \sum_{n\notin C}\int d\mathbf{r}'_n \frac{\bar{\rho}(\mathbf{r}'_n)}{|\mathbf{r}_I - \mathbf{r}'_n + \mathbf{R}_{In}|} + \sum_{n\notin C}\frac{\bar{Z}^n}{|\mathbf{r}_I + \mathbf{R}_{In}|} + v_{AB}^{xc}(\rho_{AB}(\mathbf{r}_I))$$

and

$$v_{AB}(\mathbf{r}_J) = \frac{\int d\mathbf{r}'_J \rho_{AB}(\mathbf{r}'_J)}{|\mathbf{r}_J - \mathbf{r}'_J|} + \frac{\int d\mathbf{r}'_I \rho_{AB}(\mathbf{r}'_I)}{|\mathbf{r}_J - \mathbf{r}'_I + \mathbf{R}_{JI}|} + \frac{Z_{AB}^J}{|\mathbf{r}_J|} + \frac{Z_{AB}^I}{|\mathbf{r}_J + \mathbf{R}_{JI}|} + \sum_{n\notin C}\int d\mathbf{r}'_n \frac{\bar{\rho}(\mathbf{r}'_n)}{|\mathbf{r}_J - \mathbf{r}'_n + \mathbf{R}_{Jn}|} + \sum_{n\notin C}\frac{\bar{Z}^n}{|\mathbf{r}_J + \mathbf{R}_{Jn}|} + v_{AB}^{xc}(\rho_{AB}(\mathbf{r}_J)),$$

where $Z_{AB}^I=Z_A$ and $Z_{AB}^J=Z_B$. The remaining cluster potentials follow by simply replacing AB with the appropriate cluster

configuration γ in the above formulas. The average charge and nuclear densities are given by

$$\bar{\rho}(\mathbf{r}'_n) = P(AA)\rho_{AA}(\mathbf{r}_I) + P(AB)\rho_{AB}(\mathbf{r}_I) + P(BA)\rho_{BA}(\mathbf{r}_I) + P(BB)\rho_{BB}(\mathbf{r}_I)$$

and

$$\bar{Z}^n = P(AA)Z^I_{AA} + P(AB)Z^I_{AB} + P(BA)Z^I_{BA} + P(BB)Z^I_{BB} = P(A)Z_A + P(B)Z_B,$$

where any site I in the cluster may be chosen since all sites are equivalent on average.

(v) Using the new cluster potentials $\underline{v}_{AA}(\mathbf{r})$, $\underline{v}_{AB}(\mathbf{r})$, $\underline{v}_{BA}(\mathbf{r})$, and $\underline{v}_{BB}(\mathbf{r})$, begin again from step (i) until self-consistency is achieved.

Finally note that in the above $N_c=2$ example the computational effort may be reduced since

$$\begin{aligned} v_{AA}(\mathbf{r}_I) &= v_{AA}(\mathbf{r}_J), \\ v_{AB}(\mathbf{r}_I) &= v_{BA}(\mathbf{r}_J), \\ v_{BA}(\mathbf{r}_I) &= v_{AB}(\mathbf{r}_J), \\ v_{BB}(\mathbf{r}_I) &= v_{BB}(\mathbf{r}_J), \end{aligned} \tag{F1}$$

through the use of symmetry.

APPENDIX G: EVALUATION OF LOCAL POTENTIAL AND ELECTRONIC GRAND POTENTIAL

First note that the first and second terms of Eq. (26) and the fourth and fifth terms of Eq. (29) all only involve a finite sum over cluster sites and so are straightforward to calculate. The only terms which appear to be complex to calculate compared to those in the conventional SCF-KKR-CPA theory are those involving sums which are restricted to run over all sites n outside of the cluster. However, here it is shown how these terms can be calculated using standard methods.

In order to calculate the third term of Eq. (26), note that it can be rewritten in the form

$$\begin{aligned} v^{(3)}_\gamma(\mathbf{r}_I) &= \sum_{n\notin C} \frac{\int d\mathbf{r}'_n \bar{\rho}(\mathbf{r}'_n)}{|\mathbf{r}_I - \mathbf{r}'_n + \mathbf{R}_{In}|} \\ &= \sum_m \frac{\int d\mathbf{r}'_m \bar{\rho}(\mathbf{r}'_m)}{|\mathbf{r}_I - \mathbf{r}'_m + \mathbf{R}_{Im}|} - \sum_J \frac{\int d\mathbf{r}'_J \bar{\rho}(\mathbf{r}'_J)}{|\mathbf{r}_I - \mathbf{r}'_J + \mathbf{R}_{IJ}|} \\ &= I_1 - I_2, \end{aligned} \tag{G1}$$

where m runs over all sites in the lattice and J is restricted to run over all sites in the cluster only. To calculate I_1, note that $\bar{\rho}(\mathbf{r}'_m)$ is known from Eq. (27) and the sum is over all sites m in the lattice. Therefore the standard Ewald decomposition[61] can be employed to calculate this term. I_2 may straightforwardly be calculated as the sum

$$I_2 = \sum_J \frac{\int d\mathbf{r}'_J \bar{\rho}(\mathbf{r}'_J)}{|\mathbf{r}_I - \mathbf{r}'_J + \mathbf{R}_{IJ}|} = \sum_\gamma P_\gamma \sum_J \frac{\int d\mathbf{r}'_J \rho_\gamma(\mathbf{r}'_J)}{|\mathbf{r}_I - \mathbf{r}'_J + \mathbf{R}_{IJ}|} = \sum_\gamma P_\gamma (I_3), \tag{G2}$$

where each I_3 is simply the (known) first term of Eq. (26) for each configuration γ. The calculation of the fourth term of Eq. (26) follows analogously.

Similarly, in order to calculate the sixth term in Eq. (29), note that it can be rewritten in the form

$$\begin{aligned} \Omega^{(6)} &= \frac{1}{2}\frac{1}{N_c}\sum_\gamma P_\gamma \sum_I \sum_{n\notin C} \frac{\int d\mathbf{r}_I \rho_\gamma(\mathbf{r}_I) \int d\mathbf{r}'_n \bar{\rho}(\mathbf{r}'_n)}{|\mathbf{r}_I - \mathbf{r}'_n + \mathbf{R}_{In}|} \\ &= \frac{1}{2}\frac{1}{N_c}\sum_\gamma P_\gamma \sum_I \sum_m \frac{\int d\mathbf{r}_I \rho_\gamma(\mathbf{r}_I) \int d\mathbf{r}'_m \bar{\rho}(\mathbf{r}'_m)}{|\mathbf{r}_I - \mathbf{r}'_m + \mathbf{R}_{Im}|} \\ &\quad - \frac{1}{2}\frac{1}{N_c}\sum_\gamma P_\gamma \sum_I \sum_J \frac{\int d\mathbf{r}_I \rho_\gamma(\mathbf{r}_I) \int d\mathbf{r}'_J \bar{\rho}(\mathbf{r}'_J)}{|\mathbf{r}_I - \mathbf{r}'_J + \mathbf{R}_{IJ}|} \\ &= I_4 - I_5, \end{aligned} \tag{G3}$$

where again m runs over all sites in the lattice and J is restricted to run over the cluster sites only. I_4 above can thus be calculated using the standard Ewald decomposition. I_5 is a finite sum over the cluster sites and so can be straightforwardly calculated from its present form or, alternatively, from

$$I_5 = -\frac{1}{2}\frac{1}{N_c}\sum_{\gamma,\gamma'} P_\gamma P_{\gamma'} \sum_{I,J} \frac{\int d\mathbf{r}_I \rho_\gamma(\mathbf{r}_I) \int d\mathbf{r}'_J \rho_{\gamma'}(\mathbf{r}'_J)}{|\mathbf{r}_I - \mathbf{r}'_J + \mathbf{R}_{IJ}|} \tag{G4}$$

by using Eq. (G2). The calculation of the seventh term in Eq. (29) follows analogously.

[1] P. S. Rudman, J. Stringer, and R. I. Jaffe, *Phase Stability in Metals and Alloys* (McGraw-Hill, New York, 1967).
[2] F. Ducastelle, *Order and Phase Stability in Alloys*, Vol. 3 of Cohesion and Structure (North-Holland, Amsterdam, 1991).
[3] B. L. Györffy, D. D. Johnson, F. J. Pinski, D. M. Nicholson, and G. M. Stocks, in *Proceedings of the NATO Advanced Study Institute on Alloy Phase Stability*, edited by G. M. Stocks and A. Gonis (Kluwer, Dordrecht, 1987), p. 421.
[4] J. W. D. Connolly and A. R. Williams, Phys. Rev. B **27**, R5169 (1983).
[5] J. B. Staunton, D. D. Johnson, and F. J. Pinski, Phys. Rev. B **50**, 1450 (1994).
[6] G. M. Stocks and H. Winter, Z. Phys. B: Condens. Matter **46**, 95 (1982).
[7] H. Winter and G. M. Stocks, Phys. Rev. B **27**, 882 (1983).
[8] D. D. Johnson, D. M. Nicholson, F. J. Pinski, B. L. Györffy, and G. M. Stocks, Phys. Rev. Lett. **56**, 2088 (1986).
[9] D. D. Johnson, D. M. Nicholson, F. J. Pinski, B. L. Györffy, and G. M. Stocks, Phys. Rev. B **41**, 9701 (1990).
[10] B. L. Györffy, G. M. Stocks, B. Ginatempo, D. D. Johnson, D. M. Nicholson, F. J. Pinski, J. B. Staunton, and H. Winter, Philos. Trans. R. Soc. London, Ser. A **334**, 515 (1991).
[11] P. Hohenberg and W. Kohn, Phys. Rev. **136**, B864 (1964).
[12] W. Kohn and L. J. Sham, Phys. Rev. **140**, A1133 (1965).
[13] P. Soven, Phys. Rev. **156**, 809 (1967).
[14] I. Turek, V. Drchal, J. Kudrnovsky, M. Sob, and P. Weinberger, *Electronic Structure of Disordered Alloys, Surfaces and Interfaces* (Kluwer Academic, Boston, 1997).
[15] J. L. Moran-Lopez and J. M. Sanchez, *Theory and Applications of the Cluster Variation and Path Probability Methods* (Plenum Press, New York, 1996).
[16] R. Magri, S.-H. Wei, and A. Zunger, Phys. Rev. B **42**, 11388 (1990).
[17] Z. W. Lu, S.-H. Wei, and A. Zunger, Phys. Rev. Lett. **66**, 1753 (1991).
[18] A. Zunger, in *Structural and Phase Stability of Alloys*, edited by J. L. Moran-Lopez, F. Mejia-Lira, and J. M. Sanchez (Plenum, New York, 1992), Chap. 17.
[19] A. Zunger, in *Statics and Dynamics of Alloy Phase Transformations*, Vol. 319 of NATO Advanced Study Institute Series B: Physics, edited by A. Gonis and P. E. A. Turchi (Plenum, New York, 1993).
[20] J. B. Staunton and B. L. Györffy, Rep. Prog. Phys., **57**, 1289 (1994).
[21] I. A. Abrikosov and B. Johansson, Phys. Rev. B **57**, 14164 (1998).
[22] B. L. Györffy, Phys. Rev. B **5**, 2382 (1972).
[23] G. M. Stocks, W. M. Temmerman, and B. L. Györffy, Phys. Rev. Lett. **41**, 339 (1978).
[24] Z. W. Lu, S.-H. Wei, and A. Zunger, Phys. Rev. B **44**, 10470 (1991).
[25] J. S. Faulkner, N. Y. Moghadam, Y. Wang, and G. M. Stocks, Phys. Rev. B **57**, 7653 (1998).
[26] B. Ujfalussy, J. S. Faulkner, N. Y. Moghadam, G. M. Stocks, and Y. Wang, Phys. Rev. B **61**, 12005 (2000).
[27] J. S. Faulkner, B. Ujfalussy, Nassrin Moghadam, G. M. Stocks, and Yang Wang, J. Phys.: Condens. Matter **13**, 8573 (2001).
[28] S. Pella, J. S. Faulkner, G. M. Stocks, and B. Ujfalussy, Phys. Rev. B **70**, 064203 (2004).
[29] J. S. Faulkner, Y. Wang, and G. M. Stocks, Phys. Rev. B **52**, 17106 (1995).
[30] I. A. Abrikosov, A. M. N. Niklasson, S. I. Simak, B. Johansson, A. V. Ruban, and H. L. Skriver, Phys. Rev. Lett. **76**, 4203 (1996).
[31] J. S. Faulkner, Y. Wang, and G. M. Stocks, Phys. Rev. B **55**, 7492 (1997).
[32] A. V. Ruban and H. L. Skriver, Phys. Rev. B **66**, 024201 (2002).
[33] A. V. Ruban, S. I. Simak, P. A. Korzhavyi, and H. L. Skriver, Phys. Rev. B **66**, 024202 (2002).
[34] M. Jarrell and H. R. Krishnamurthy, Phys. Rev. B **63**, 125102 (2001).
[35] D. A. Rowlands, J. Phys.: Condens. Matter **18**, 3179-3195 (2006).
[36] D. A. Rowlands, Ph.D. thesis, University of Warwick, 2004.
[37] D. A. Rowlands, J. B. Staunton, and B. L. Györffy, Phys. Rev. B **67**, 115109 (2003).
[38] D. A. Rowlands, J. B. Staunton, B. L. Györffy, E. Bruno, and B. Ginatempo, Phys. Rev. B **72**, 045101 (2005).
[39] N. Stefanou, P. J. Braspenning, R. Zeller, and P. H. Dederichs, Phys. Rev. B **36**, 6372 (1987).
[40] N. Stefanou, R. Zeller, and P. H. Dederichs, Solid State Commun. **62**, 735 (1987).
[41] B. L. Györffy, Phys. Scr. **T49**, 373 (1993).
[42] D. A. Rowlands *et al.* (unpublished).
[43] M. H. Hettler, A. N. Tahvildar-Zadeh, M. Jarrell, Th. Pruschke, and H. R. Krishnamurthy, Phys. Rev. B **58**, R7475 (1998).
[44] M. H. Hettler, M. Mukherjee, M. Jarrell, and H. R. Krishnamurthy, Phys. Rev. B **61**, 12739 (2000).
[45] A. Gonis, *Green Functions for Ordered and Disordered Systems*, Vol. 4 of Studies in Mathematical Physics (North-Holland, Amsterdam, 1992).
[46] A. Gonis, G. M. Stocks, W. H. Butler, and H. Winter, Phys. Rev. B **29**, 555 (1984).
[47] J. S. Faulkner and G. M. Stocks, Phys. Rev. B **21**, 3222 (1980).
[48] P. Lloyd and P. R. Best, J. Phys. C **8**, 3752 (1975).
[49] B. L. Györffy and G. M. Stocks, in *Electrons in Disordered Metals and at Metallic Surfaces*, edited by P. Phariseau, B. L. Györffy, and L. Scheire (Plenum, New York, 1974), p. 89.
[50] D. D. Johnson and F. J. Pinski, Phys. Rev. B **48**, 11553 (1993).
[51] P. A. Korzhavyi, A. V. Ruban, I. A. Abrikosov, and H. L. Skriver, Phys. Rev. B **51**, 5773 (1995).
[52] A. Gonis, P. E. A. Turchi, J. Kudrnovsky, V. Drchal, and I. Turek, J. Phys.: Condens. Matter **8**, 7883 (1996).
[53] L. Vitos, J. Kollar, and H. L. Skriver, Phys. Rev. B **55**, 13521 (1997).
[54] M. Lüders, A. Ernst, M. Däne, Z. Szotek, A. Svane, D. Ködderitzsch, W. Hergert, B. L. Györffy, and W. M. Temmerman, Phys. Rev. B **71**, 205109 (2005).
[55] H. Akai and P. H. Dederichs, Phys. Rev. B **47**, 8739 (1993).
[56] M. Weinert, E. Wimmer, and A. J. Freeman, Phys. Rev. B **26**, 4571 (1982).
[57] C. Wolverton, Alex Zunger, S. Froyen, and S.-H. Wei, Phys. Rev. B **54**, 7843 (1996).
[58] R. J. Cole, N. J. Brooks, and P. Weightman, Phys. Rev. Lett. **78**, 3777 (1997).
[59] J. B. Staunton and B. L. Györffy, Phys. Rev. Lett. **69**, 371 (1992).
[60] A. Messiah, in *Quantum Mechanics*, edited by G. M. Temmer (North-Holland, Amsterdam, 1963), p. 404.
[61] P. P. Ewald, Ann. Phys. (N.Y.) **64**, 253 (1921).